Relaxion dark matter & tabletop exp.

Gilad Perez

Weizmann Inst.

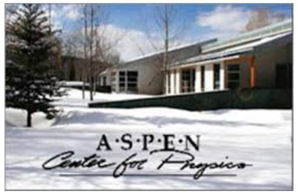

In Pursuit of New Particles and Paradigms

Aspen, Winter 2019

Outline

- Intro.: Relaxion & the naturalness-log-crisis.
- Coherent relaxion DM \w dynamical misalignment =>
  time-variation of constant of nature.
- Probing heavyish-light-scalar/relaxion DM \w clocks.
- Probing scalar-stars \w clocks (earth & space).
- Conclusions.

The relaxion mechanism & the hier' problem

Graham, Kaplan & Rajendran (15)

(*i*) Add a scalar (relaxion) Higgs dependent mass: $$(\overbrace{\Lambda^2 - g^2\phi^2}^{\mu^2(\phi)})\, H^\dagger H.$$

(*ii*) Introduce a "rolling" potential for the relaxion.

(*iii*) Add a "backreacion" moguls (wiggly potential) for the relaxion.

The relaxion mechanism & the hier’ problem

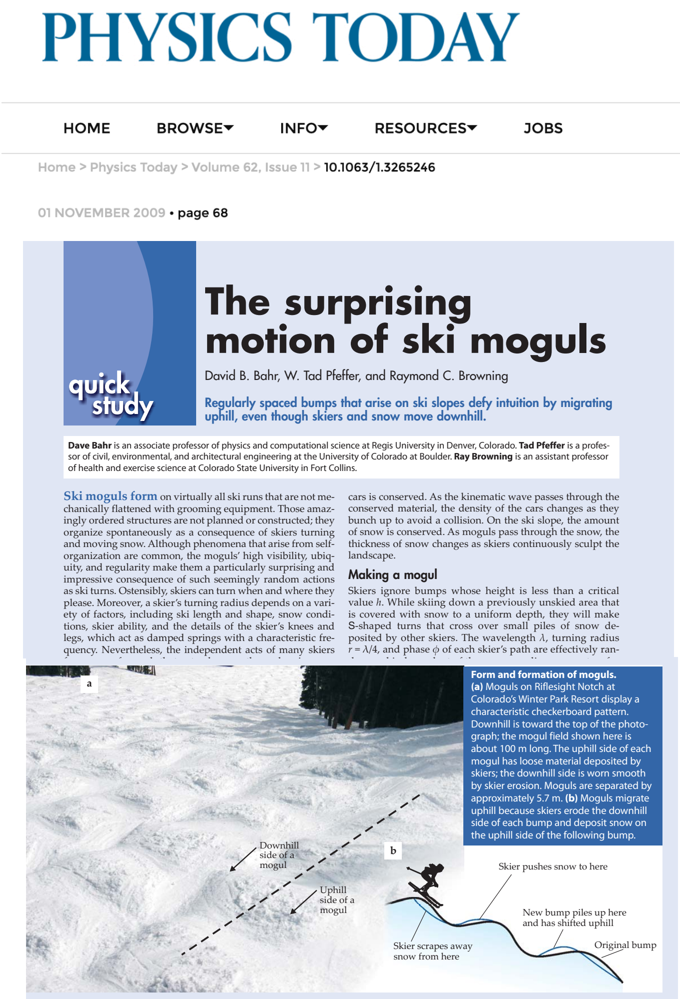

PHYSICS TODAY

HOME BROWSE INFO RESOURCES JOBS

Home > Physics Today > Volume 62, Issue 11 > 10.1063/1.3265246

01 NOVEMBER 2009 • page 68

quick study

The surprising motion of ski moguls

David B. Bahr, W. Tad Pfeffer, and Raymond C. Browning

Regularly spaced bumps that arise on ski slopes defy intuition by migrating uphill, even though skiers and snow move downhill.

Dave Bahr is an associate professor of physics and computational science at Regis University in Denver, Colorado. **Tad Pfeffer** is a professor of civil, environmental, and architectural engineering at the University of Colorado at Boulder. **Ray Browning** is an assistant professor of health and exercise science at Colorado State University in Fort Collins.

Ski moguls form on virtually all ski runs that are not mechanically flattened with grooming equipment. Those amazingly ordered structures are not planned or constructed; they organize spontaneously as a consequence of skiers turning and moving snow. Although phenomena that arise from self-organization are common, the moguls’ high visibility, ubiquity, and regularity make them a particularly surprising and impressive consequence of such seemingly random actions as ski turns. Ostensibly, skiers can turn when and where they please. Moreover, a skier’s turning radius depends on a variety of factors, including ski length and shape, snow conditions, skier ability, and the details of the skier’s knees and legs, which act as damped springs with a characteristic frequency. Nevertheless, the independent acts of many skiers

cars is conserved. As the kinematic wave passes through the conserved material, the density of the cars changes as they bunch up to avoid a collision. On the ski slope, the amount of snow is conserved. As moguls pass through the snow, the thickness of snow changes as skiers continuously sculpt the landscape.

Making a mogul

Skiers ignore bumps whose height is less than a critical value h. While skiing down a previously unskied area that is covered with snow to a uniform depth, they will make S-shaped turns that cross over small piles of snow deposited by other skiers. The wavelength λ, turning radius $r = \lambda/4$, and phase ϕ of each skier’s path are effectively ran-

Form and formation of moguls. **(a)** Moguls on Riflesight Notch at Colorado’s Winter Park Resort display a characteristic checkerboard pattern. Downhill is toward the top of the photograph; the mogul field shown here is about 100 m long. The uphill side of each mogul has loose material deposited by skiers; the downhill side is worn smooth by skier erosion. Moguls are separated by approximately 5.7 m. **(b)** Moguls migrate uphill because skiers erode the downhill side of each bump and deposit snow on the uphill side of the following bump.

(iv) The moguls height depend on Higgs VEV, they grow till minima is created, which stops the relaxion when $\langle H\rangle \sim 10^2\,\mathrm{GeV} \ll \Lambda$.

Relaxion mechanism (inflation based)

Graham, Kaplan & Rajendran (15)

(i) Add a scalar (relaxion) Higgs dependent mass: $\overbrace{(\Lambda^2 - g^2\phi^2)}^{\mu^2(\phi)}\, H^\dagger H$

(ii) ϕ roles till μ^2 changes sign $\Rightarrow \langle H \rangle \neq 0 \Rightarrow$ stops rolling.

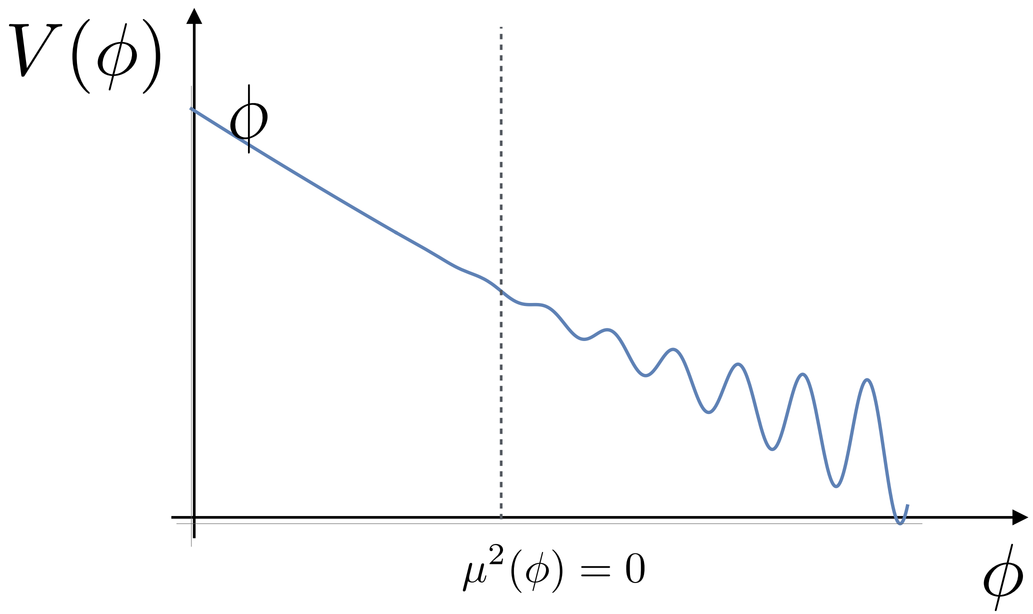

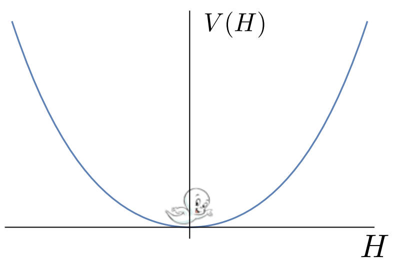

Relaxion mechanism (inflation based)

Graham, Kaplan & Rajendran (15)

(i) Add a scalar (relaxion) Higgs dependent mass: $\overbrace{(\Lambda^2 - g^2\phi^2)}^{\mu^2(\phi)} H^\dagger H$

(ii) ϕ roles till μ^2 changes sign $\Rightarrow \langle H \rangle \neq 0 \Rightarrow$ stops rolling.

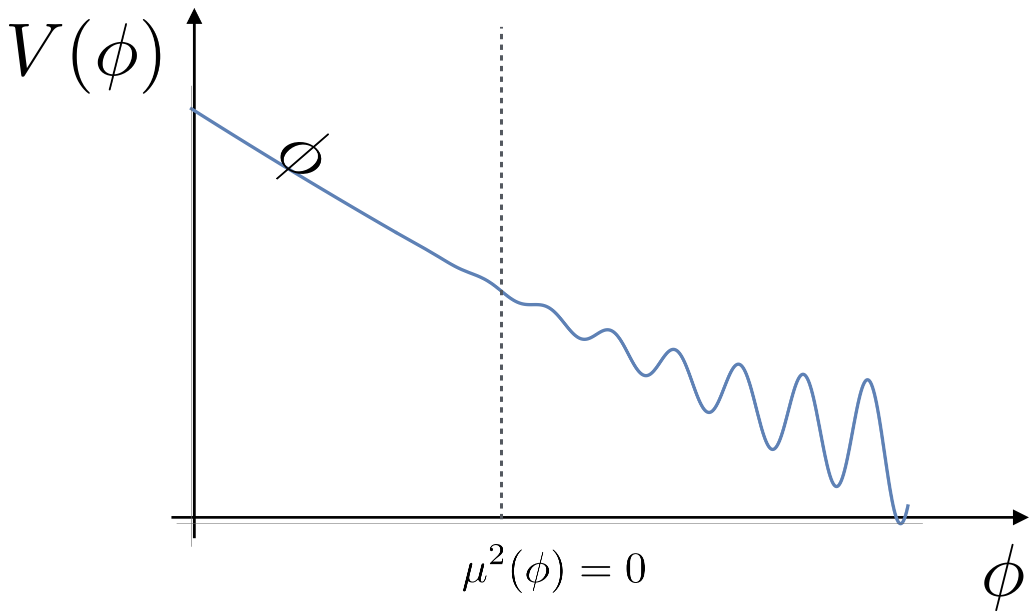

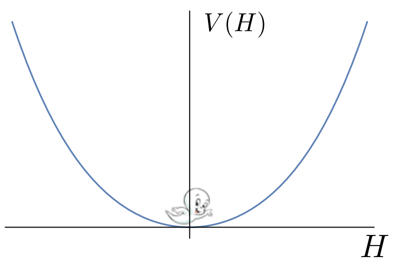

Relaxion mechanism (inflation based)

Graham, Kaplan & Rajendran (15)

(i) Add a scalar (relaxion) Higgs dependent mass: $\overbrace{(\Lambda^2 - g^2\phi^2)}^{\mu^2(\phi)} H^\dagger H$

(ii) ϕ roles till μ^2 changes sign $\Rightarrow \langle H \rangle \neq 0 \Rightarrow$ stops rolling.

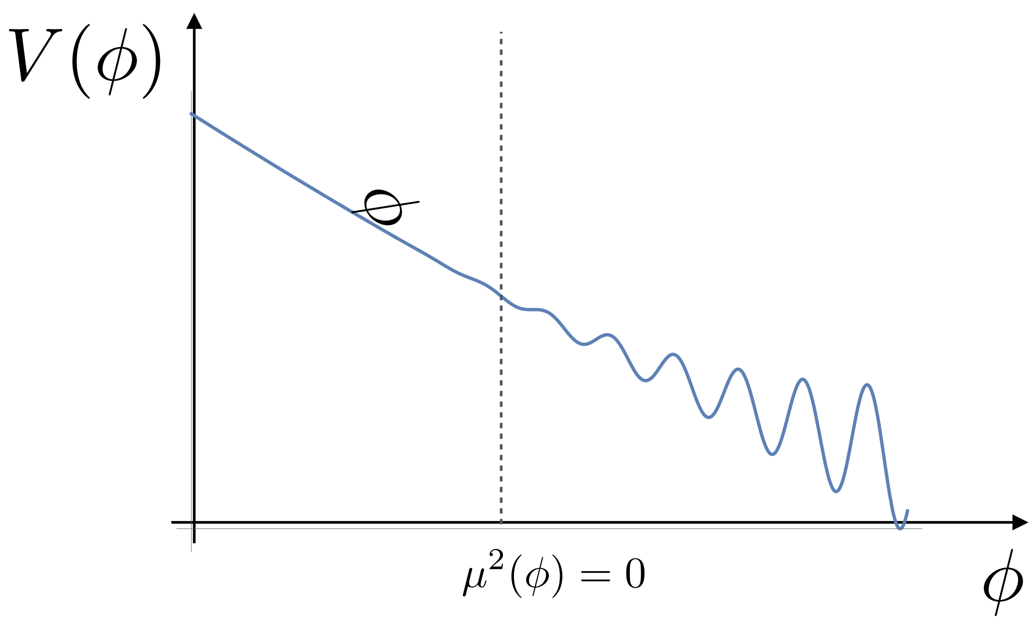

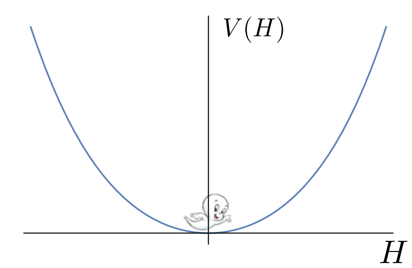

Relaxion mechanism (inflation based)

Graham, Kaplan & Rajendran (15)

(i) Add a scalar (relaxion) Higgs dependent mass: $\left(\overbrace{\Lambda^2 - g^2\phi^2}^{\mu^2(\phi)}\right) H^\dagger H$

(ii) ϕ roles till μ^2 changes sign $\Rightarrow \langle H \rangle \neq 0 \Rightarrow$ stops rolling.

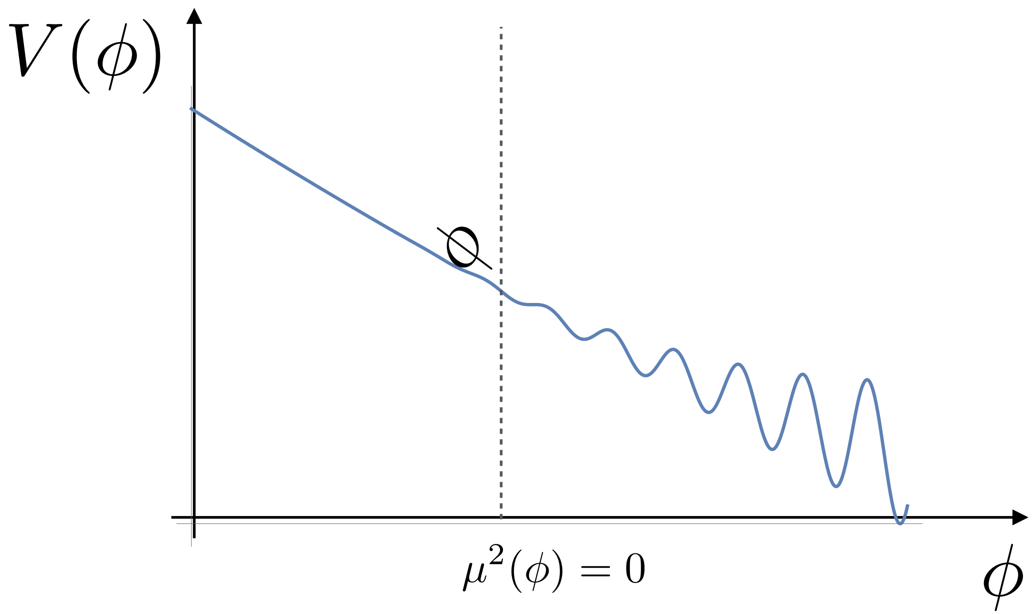

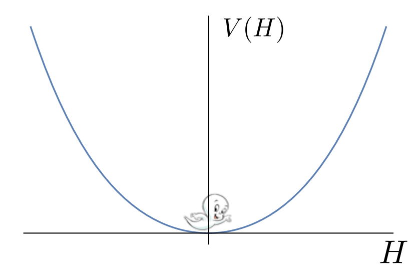

Relaxion mechanism (inflation based)

Graham, Kaplan & Rajendran (15)

(i) Add a scalar (relaxion) Higgs dependent mass: $\overbrace{(\Lambda^2 - g^2\phi^2)}^{\mu^2(\phi)}\, H^\dagger H$

(ii) ϕ roles till μ^2 changes sign $\Rightarrow \langle H \rangle \neq 0 \Rightarrow$ stops rolling.

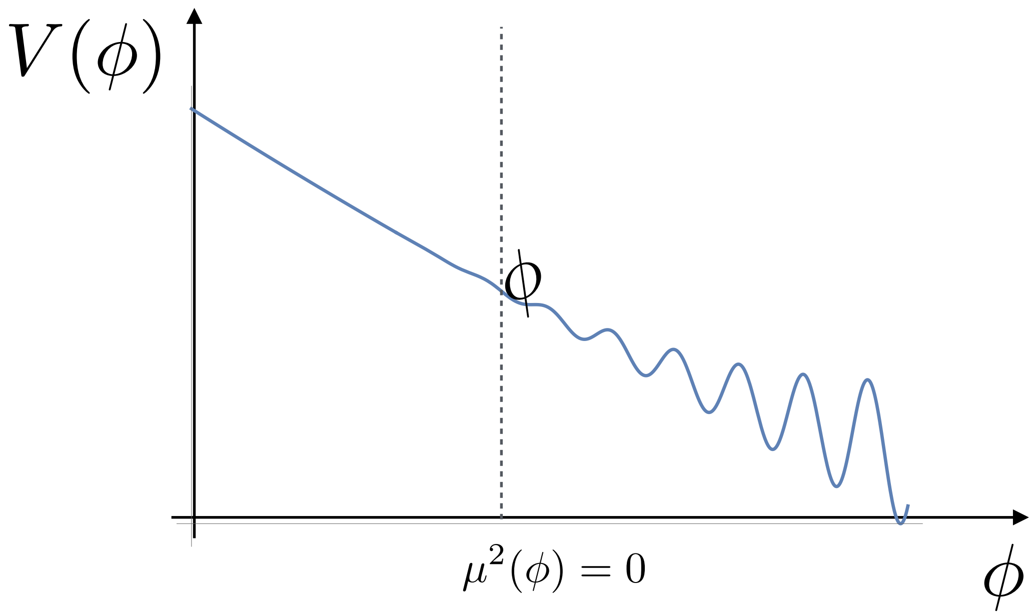

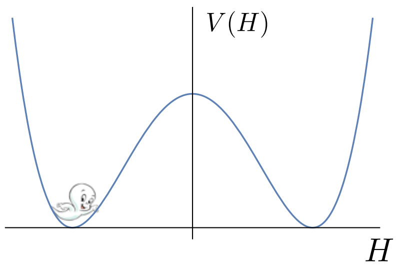

Relaxion mechanism (inflation based)

Graham, Kaplan & Rajendran (15)

(*i*) Add a scalar (relaxion) Higgs dependent mass: $\overbrace{(\Lambda^2 - g^2\phi^2)}^{\mu^2(\phi)}\, H^\dagger H$

(ii) ϕ roles till μ^2 changes sign $\Rightarrow \langle H \rangle \neq 0 \Rightarrow$ stops rolling.

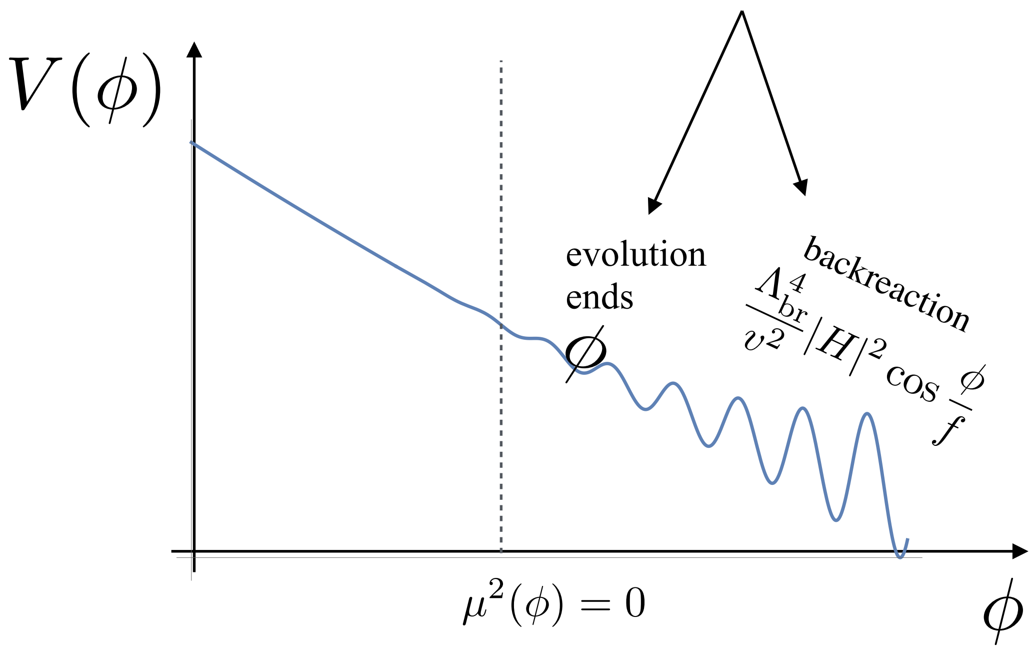

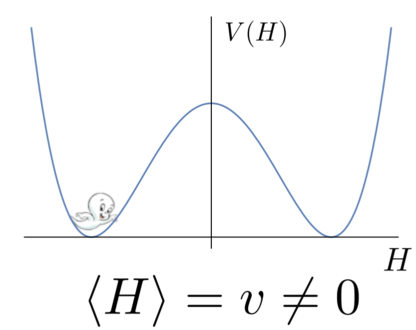

Summary relaxion physics

- A dynamical solution/amelioration of the Higgs fine-tuning problem.

- Focus shifts from TeV Higgs dynamics to relaxion, which is a weird axion, naturally light & weakly coupled …

- As the minimum of the backreaction potential is not at zero => spontaneous CP violation is induced => QCD CP problem can be solved a la Nelson-Barr (or by giving-up on classical evolution …)

Davidi, Gupta, GP, Redigolo & Shalit; Gupta; Nelson & Prescod-Weinstein (17)

- CP violation => relaxion-Higgs mixing => rich pheno'.

Flacke, Frugiuele, Fuchs, Gupta & GP; Choi & Im (16)

Hunting the relaxion & naturalness log-crisis

Frugiuele, Fuchs, GP & Schlaffer (18)

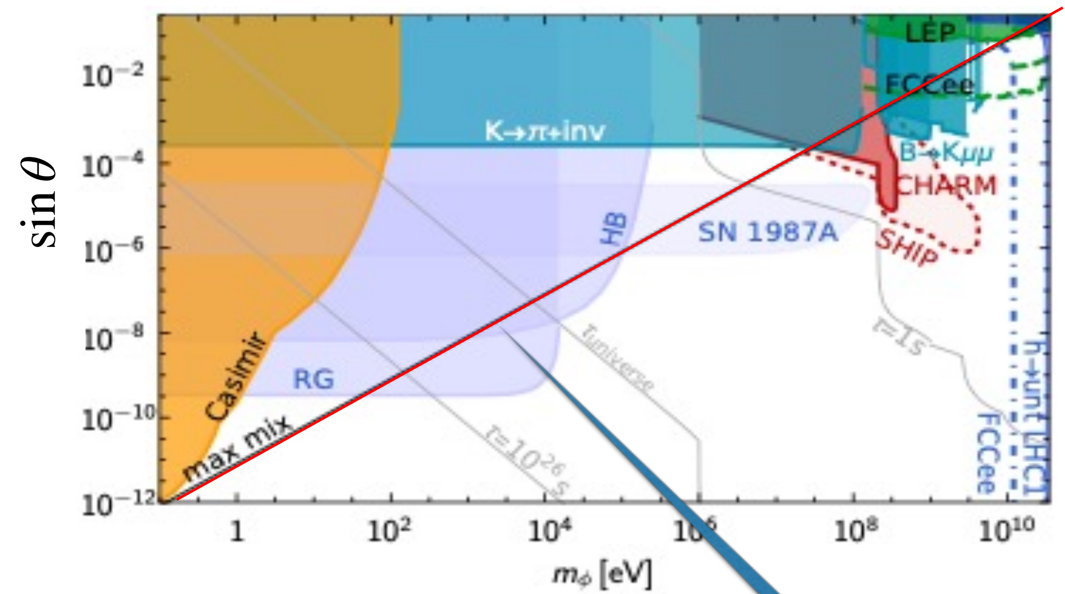

"Physical" region: below diagonal

Aharony, Akerman, Ozeri, GP, Savoray, Shaniv;
Banerjee, Budker, Eby, Kim & GP (19)
Antypas, Tretiak, Garcon, Ozeri, GP & Budker,to appear

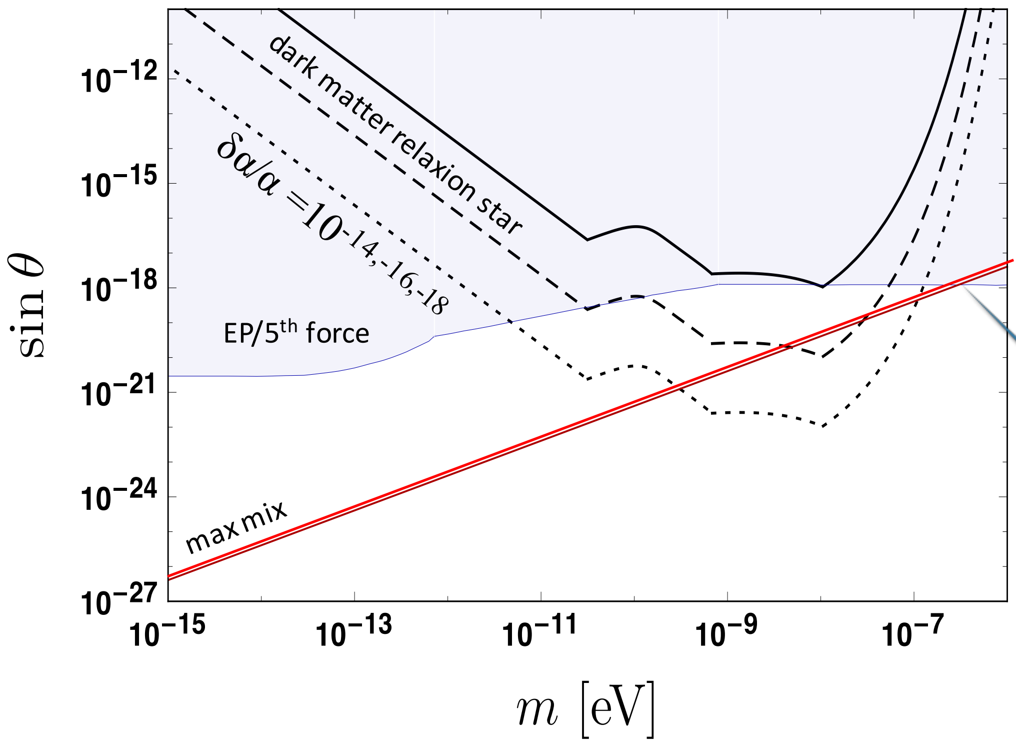

"Physical" region: below diagonal

Relaxion/scalar light dark matter

Banerjee, Kim & GP (18)

Concrete ex.: relaxion dark matter (DM)

Banerjee, Kim & GP (18)

- Basic idea is similar to axion DM (but avoiding missalignment problem):

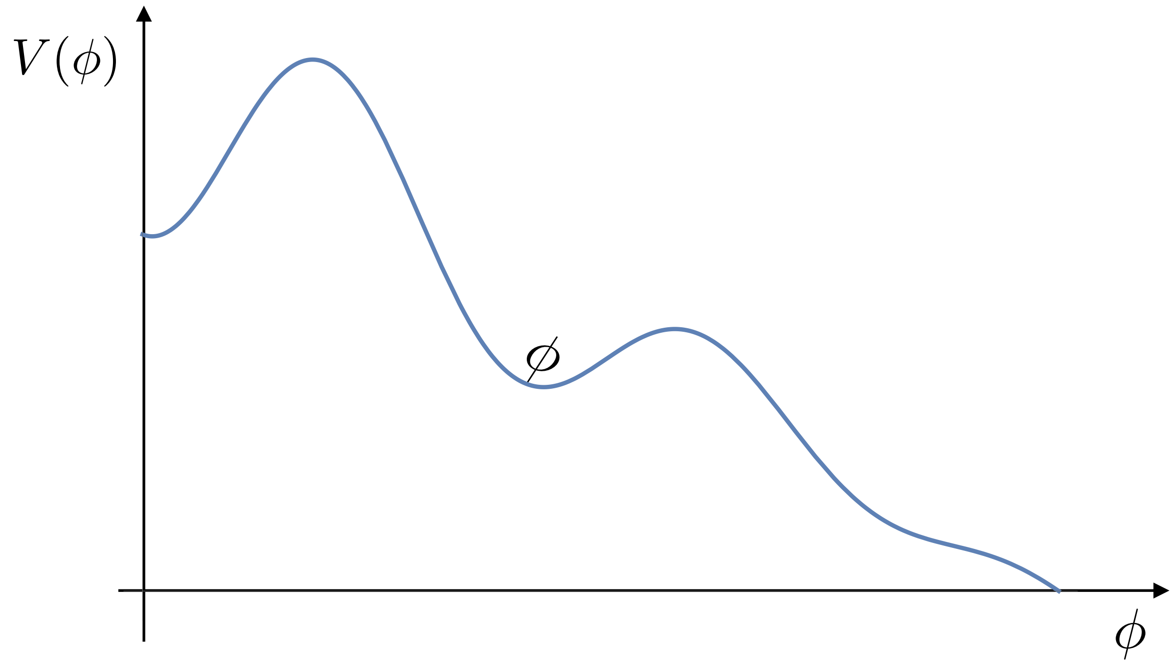

Concrete ex.: relaxion dark matter (DM)

- Basic idea is similar to axion DM (but avoiding missalignment problem):

  After reheating the wiggles disappear (sym' restoration):

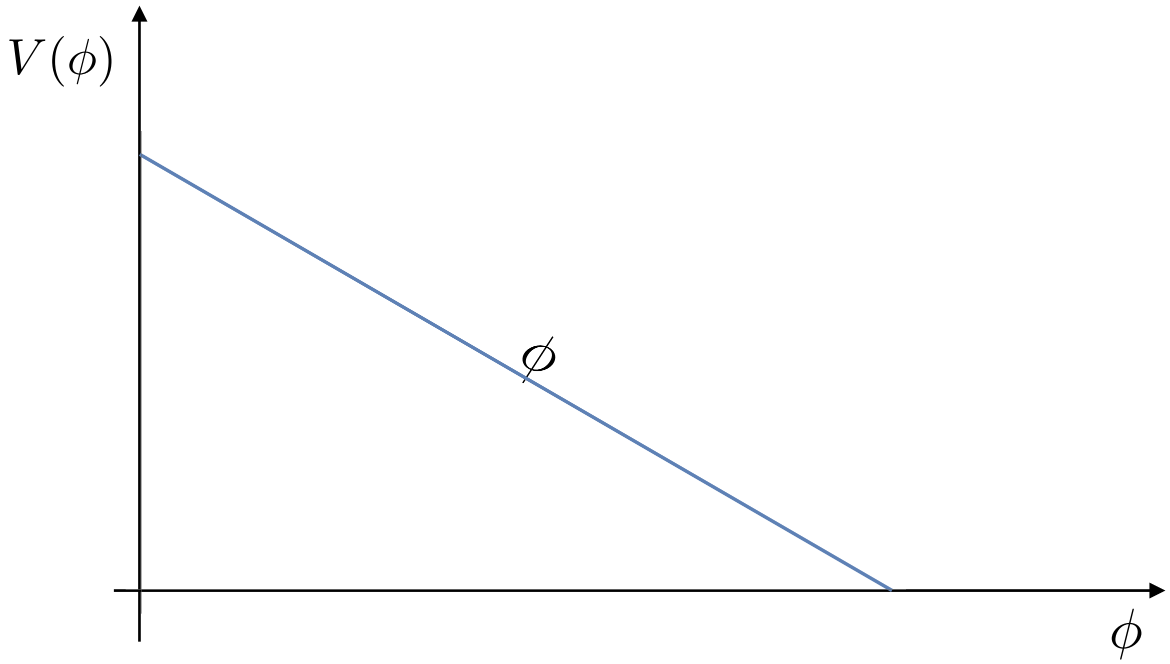

Concrete ex.: relaxion dark matter (DM)

- Basic idea is similar to axion DM (but avoiding missalignment problem):

  After reheating the wiggles disappear: and the relaxion roles a bit.

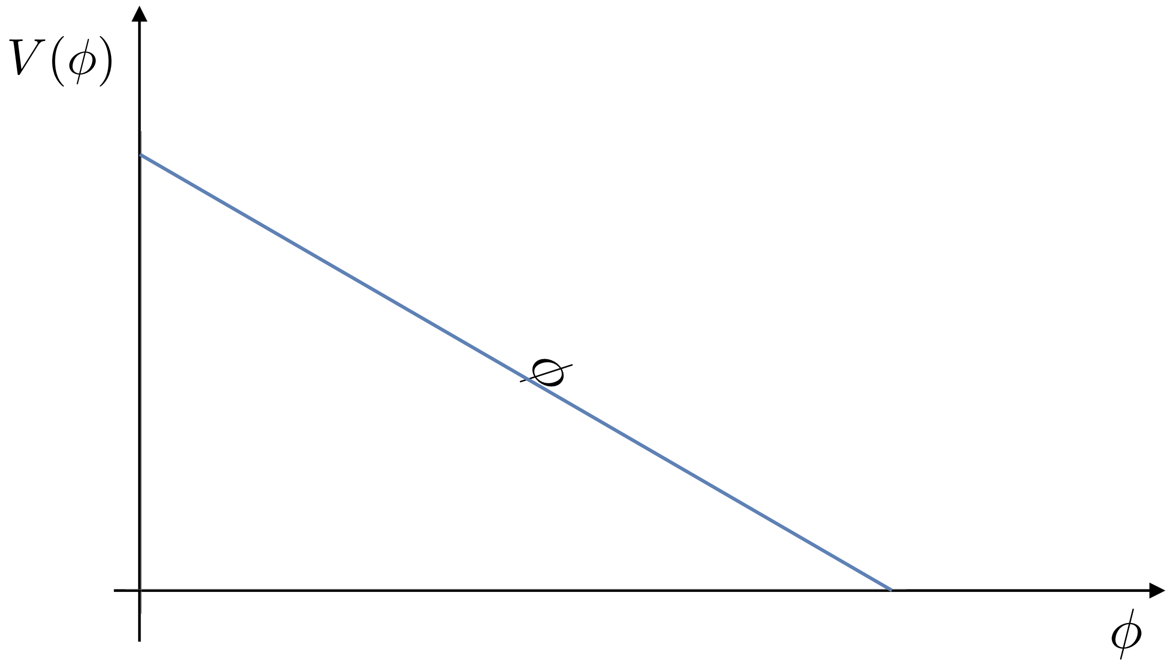

Concrete ex.: relaxion dark matter (DM)

- Basic idea is similar to axion DM (but avoiding missalignment problem):

  After reheating the wiggles disappear: and the relaxion roles a bit.

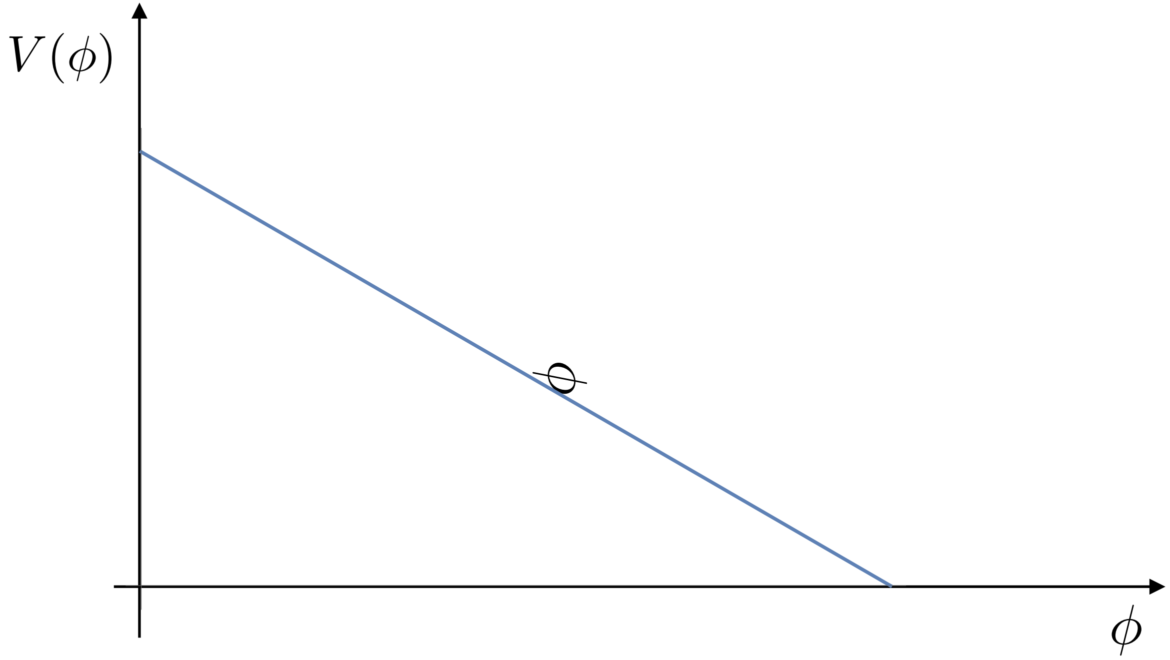

Concrete ex.: relaxion dark matter (DM)

- Basic idea is similar to axion DM (but avoiding missalignment problem):

  Now the relaxion not at the min' and start to oscillates = DM.

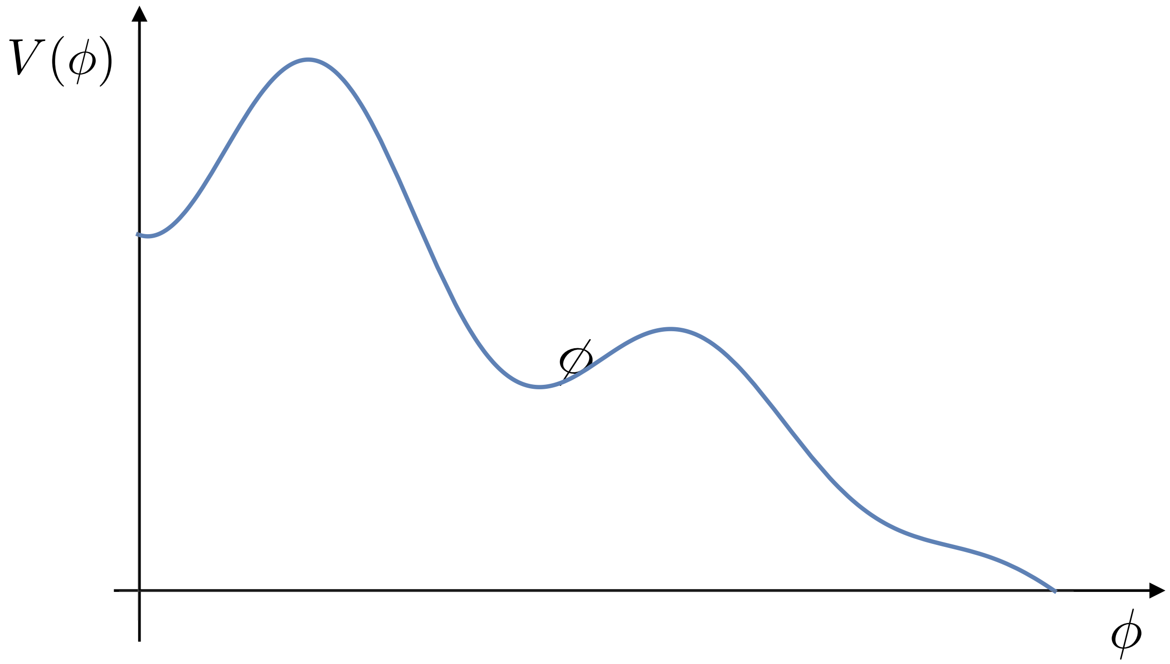

Concrete ex.: relaxion dark matter (DM)

- Basic idea is similar to axion DM (but avoiding missalignment problem):

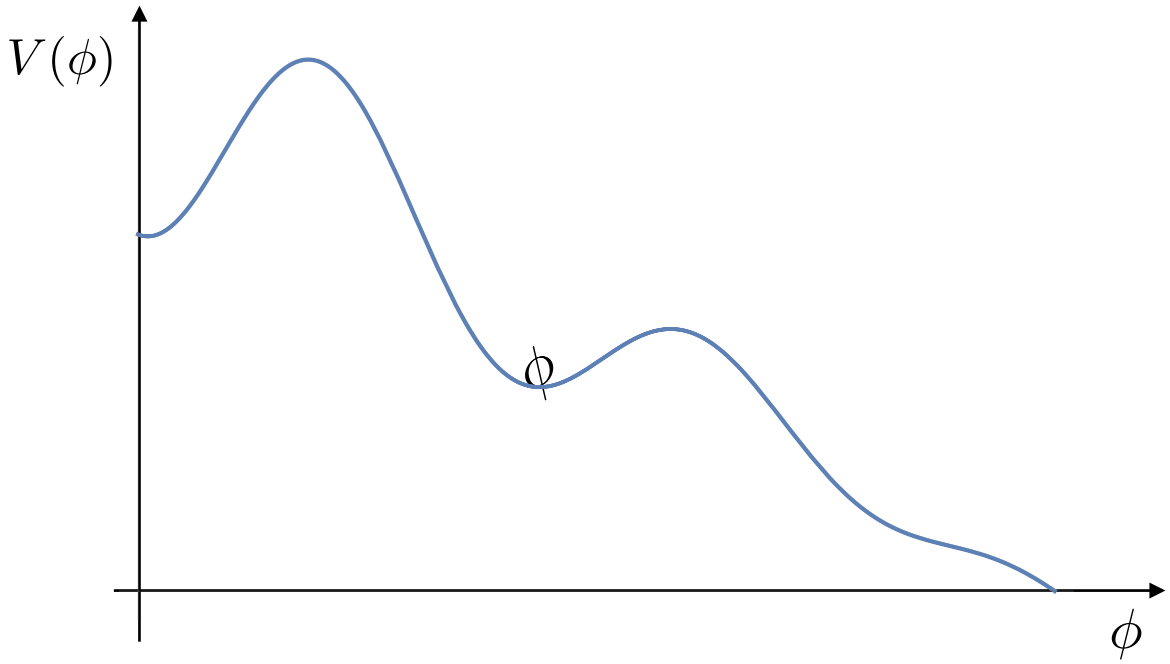

Concrete ex.: relaxion dark matter (DM)

- Basic idea is similar to axion DM (but avoiding missalignment problem):

  Now the relaxion not at the min' and start to oscillates = DM.

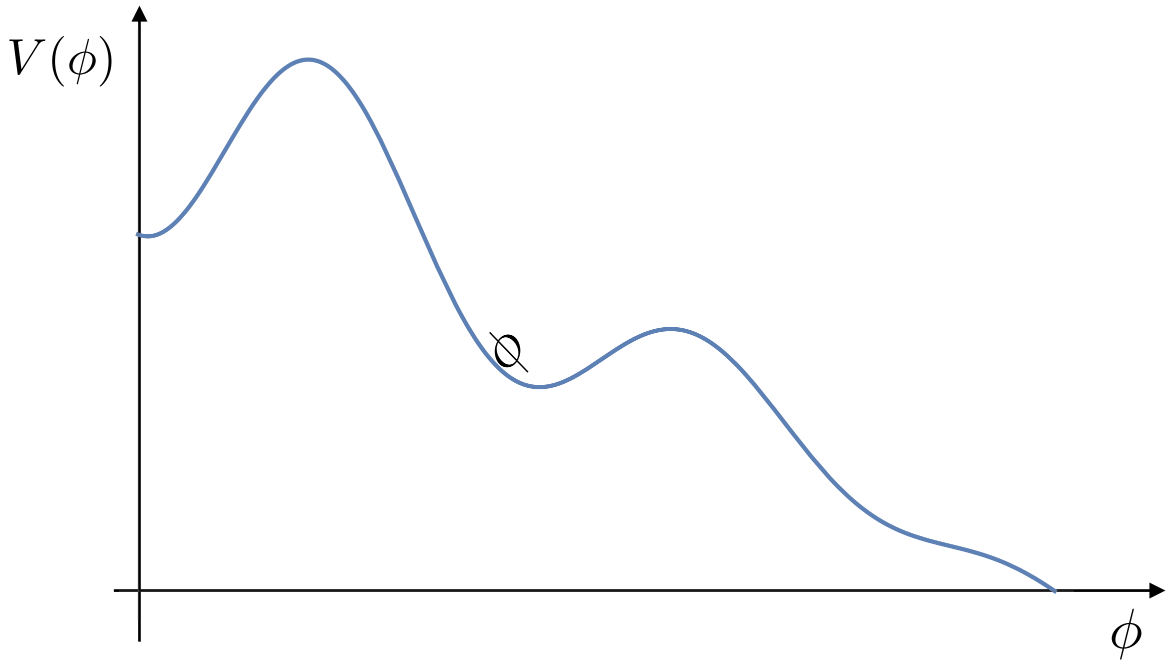

Concrete ex.: relaxion dark matter (DM)

- Basic idea is similar to axion DM (but avoiding missalignment problem):

  Now the relaxion not at the min' and start to oscillates = DM.

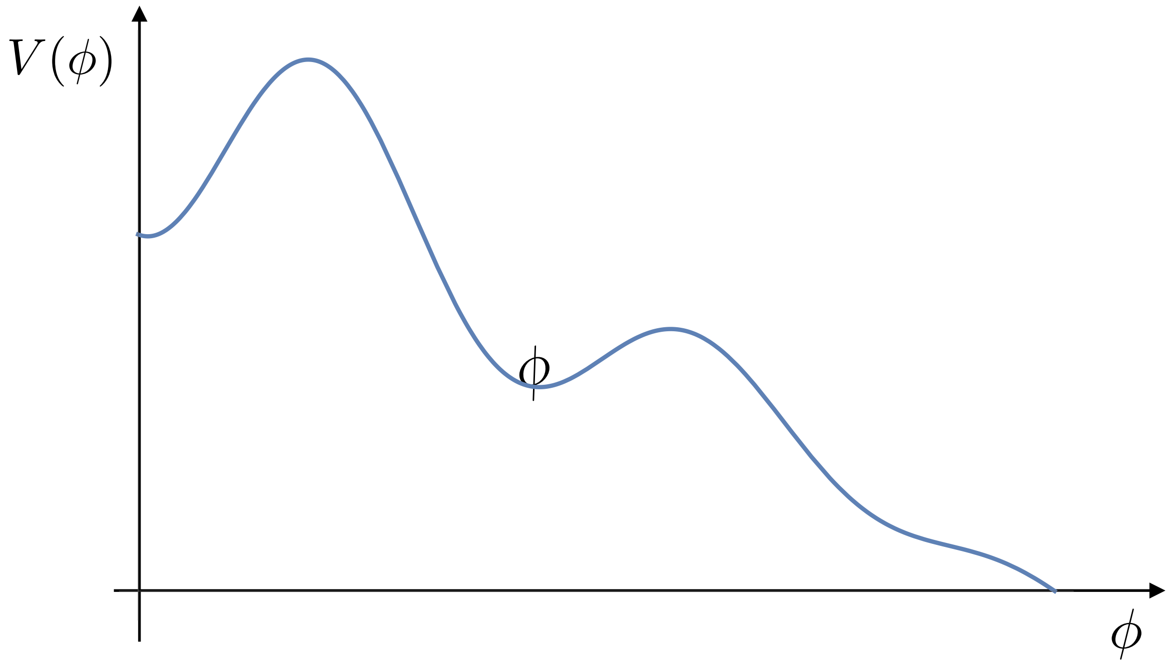

Concrete ex.: relaxion dark matter (DM)

- Basic idea is similar to axion DM (but avoiding missalignment problem):

  Now the relaxion not at the min' and start to oscillates = DM.

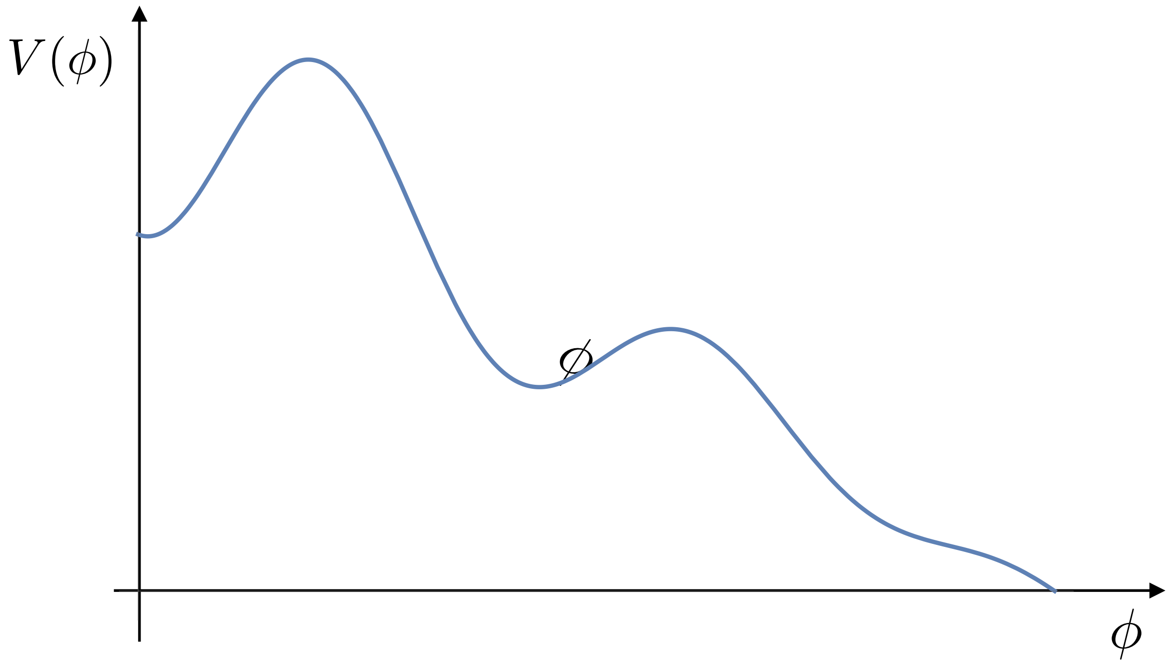

Coherent relaxion DM relic density

- Basic idea is similar to axion DM (but avoiding missalignment problem):

  Now the relaxion not at the min' and start to oscillates = DM.

Light-coherent DM abundance: $\rho_{\rm DM}^{\rm cos} \sim m^2 \Delta\phi^2$

For $m_\phi \gtrsim H(T_{\rm ra})$: $\rho_{\rm DM}^{\rm cos} \sim \Omega_\phi h^2 \approx 3 \times (\Delta\theta)^2_{T=T_{\rm os}} \left(\frac{\Lambda_{\rm br}}{1\,{\rm GeV}}\right)^4 \left(\frac{100\,{\rm GeV}}{T_{\rm os}}\right)^3$

where the observed DM abundance is $\Omega_{\rm DM} h^2 \simeq 0.12$

For $m_\phi < H(T_{\rm ra})$: extra suppression is obtained as oscilation starts when $H(T_{\rm osc}) \sim m_\phi$.

Relaxion dark matter, parameter space

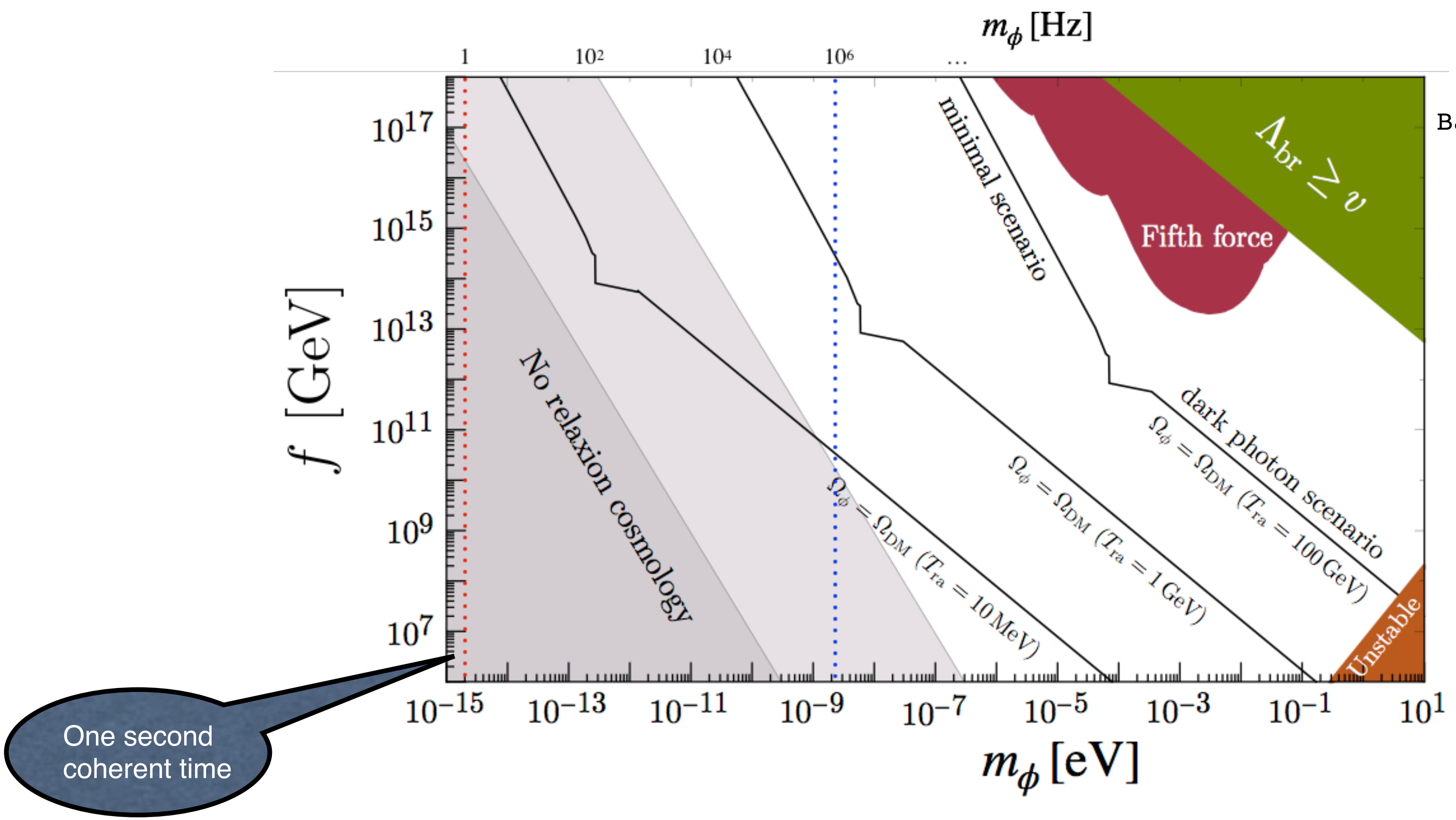

Banerjee, Kim & GP (18)

- The relaxion oscillates & mixes with the Higgs, Banerjee, Kim & GP (18)

therefore *all constants of nature + masses vary with time*.

$$\frac{\delta m_e}{m_e} \lesssim y_e \sin_{\phi h} \frac{\sqrt{\rho_{\rm DM}}}{m_e m_\phi} \sin\left(m_\phi t\right)$$

Arvanitaki, Huang & Van Tilburg (15)

Two relevant questions

(i) Notice that relevant models have osc. freq. 1 - 10^{14} Hz.
Can we probe these?

(ii) Is the amplitude large enough to probe meaningful models?

The challenging super-Hz-DM mass

Graham, Kaplan, Mardon, Rajendran & Terrano; Arvanitaki, Dimopoulos & Van Tilburg; Van Tilburg, Leefer, Bougas & Budker (15)

GP, Redigolo, Safronova, Ubaldi & Zupan, in preparation.

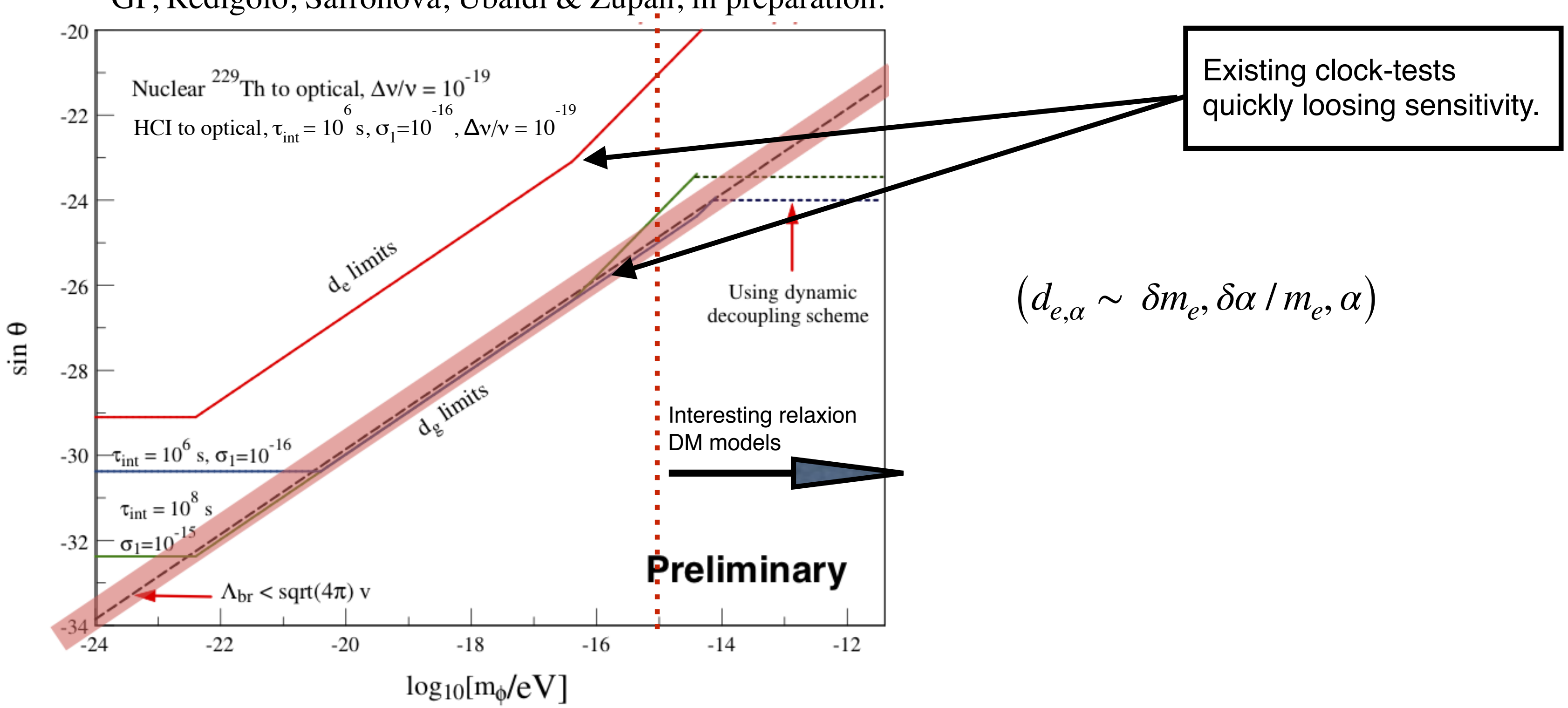

$$\left(d_{e,\alpha} \sim \ \delta m_e, \delta\alpha \,/\, m_e, \alpha\right)$$

d_e stands for the time dependent component of the fine coupling constant, the bound on d_g (the coefficient of the time dependent component of α_s, the strong coupling) assumes a working ^{229}Th nuclear clock with a 1 : 10^{19} precision, τ_{int} stands for the total assumed integration time and σ_1 stands for the corresponding stability. The dashed-red line on the diagonal corresponds to the maximal mixing allowed in this scenario, Λ_{br} corresponds to a coupling in the relaxion model.

Back to the two questions

(i) Notice that relevant models have osc. freq. 1 - 10^{14} Hz. Can we probe these?

Yes see 2 new exp' that probe this region.

(ii) Is the amplitude large enough to probe meaningful models?

However, gravity can help: dark matter might form "relaxion-planets" that might be trapped around earth-gravitational field.

Banerjee, Budker, Eby, Kim & GP (19)

(similar to axion-stars requiring stability and assuming capturing & coherence)

Kimball, et al. (17)

Method 1: Super Hz DM mass \w dynamical decoupling (DD)

Ravid Shaniv & **Roee Ozeri**

Quantum lock-in force sensing using optical clock Doppler velocimetry

Nature Communications volume 8, Article number: 14157 (2017)

An efficient method of measuring an oscillating signal by a quantum probe, in the presence of noise, is the Quantum lock-in technique. Here, a probe superposition is time modulated by a Hamiltonian term, that does not commute with the noise and signal operators. The resulting *dynamics decouples* the probe phase evolution from any frequency component that does not spectrally overlap with the probe modulation and enables a significant prolongation of the probe coherence. **On the other hand, frequency components that match some part of the modulation spectrum yield a phase that accumulates as the probe evolves with time.** If the desired signal spectrally overlaps with the probe modulation, it imprints a coherently accumulated phase signal that can be subsequently measured. This laser frequency matched the clock dipole-transition $5S_{1/2} \rightarrow 4D_{5/2}$ of a single $88Sr^{+}$ ion, on which the DD sequence was applied. Here, ν = 1013 Hz was chosen.

Effective 2-state system: $$\psi(t) = \frac{1}{\sqrt{2}}\left(\left|S, -\frac{1}{2}\right\rangle + e^{i\phi_{\text{clk}}(t)}\left|D, \frac{1}{2}\right\rangle\right),$$

Beyond 1Hz DM mass \w dynamical decoupling (DD)

Aharony, Akerman, Ozeri, GP, Shaniv & Savoray, (ion-cavity comparison) 2019

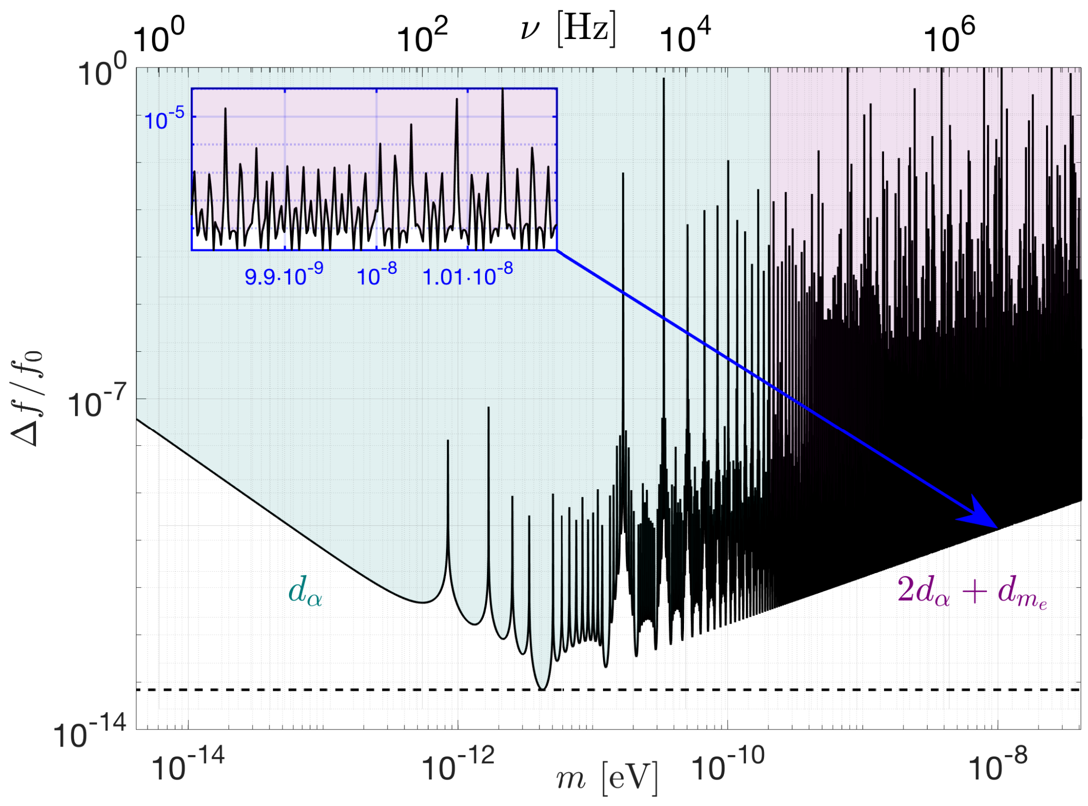

Current bound on the relative modulation of the transition frequency from a DD experiment, placed at 95% CL. The dashed line marks the current sensitivity reach, corresponding to scanning over ν_m. The inset is a magnified view of $m \sim 10^{-8}$eV.

Beyond 1Hz DM mass \w dynamical decoupling

Aharony, Akerman, Ozeri, GP & Shaniv & Savoray, 19 (ion-cavity comparison)

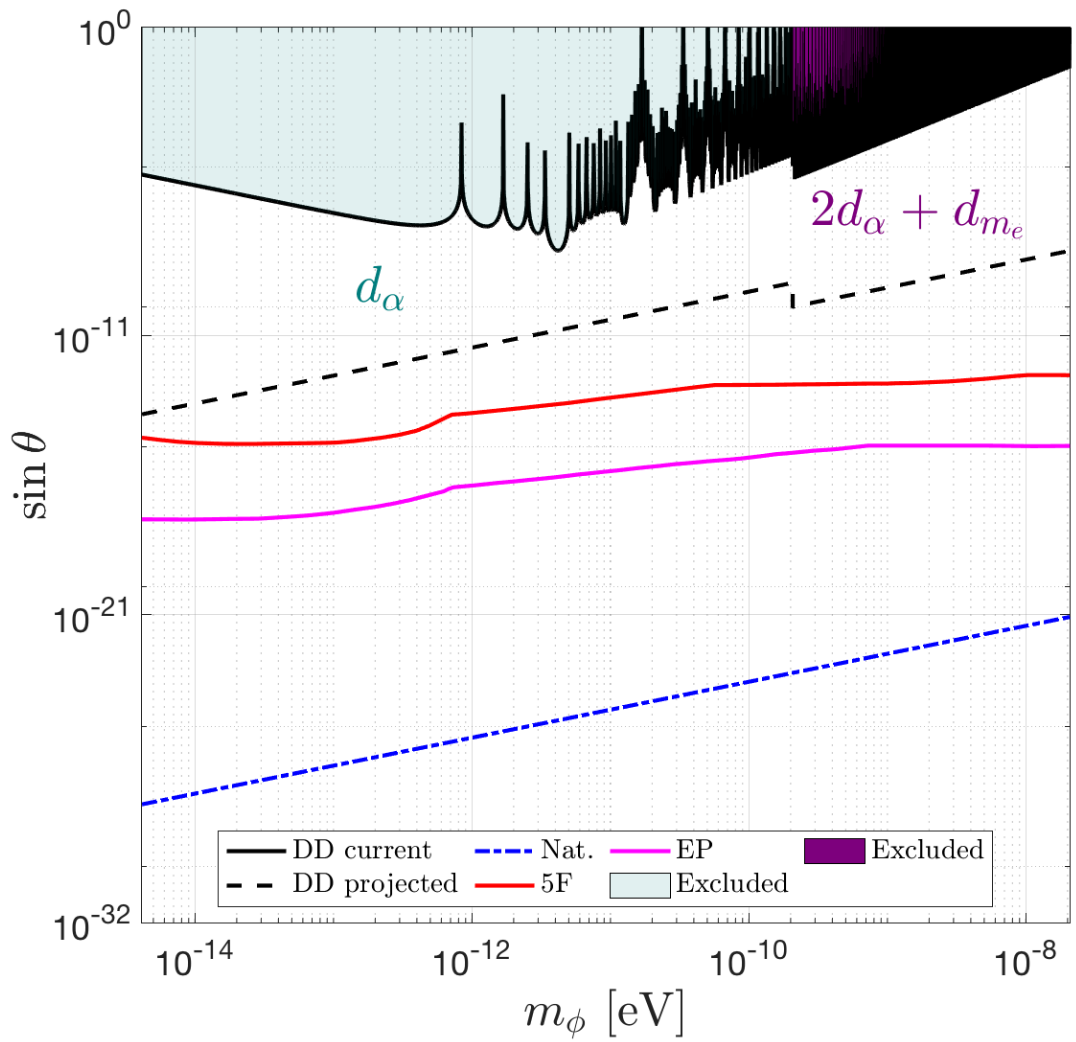

The bounds on the mixing angle of a relaxion DM: Black – current and projected bounds from DD experiments at 95% CL. Red – Bounds from fifth force experiments. Magenta – EP-tests bounds. Dash-dotted – Bounds from Naturalness.

Beyond 1Hz DM mass \w polarization spectroscopy

Antypas, Tretiak, Garcon, Ozeri, GP & Budker, to appear

Cs $6S_{1/2} \rightarrow 6P_{3/2}$ transition frequency (10 GHz)

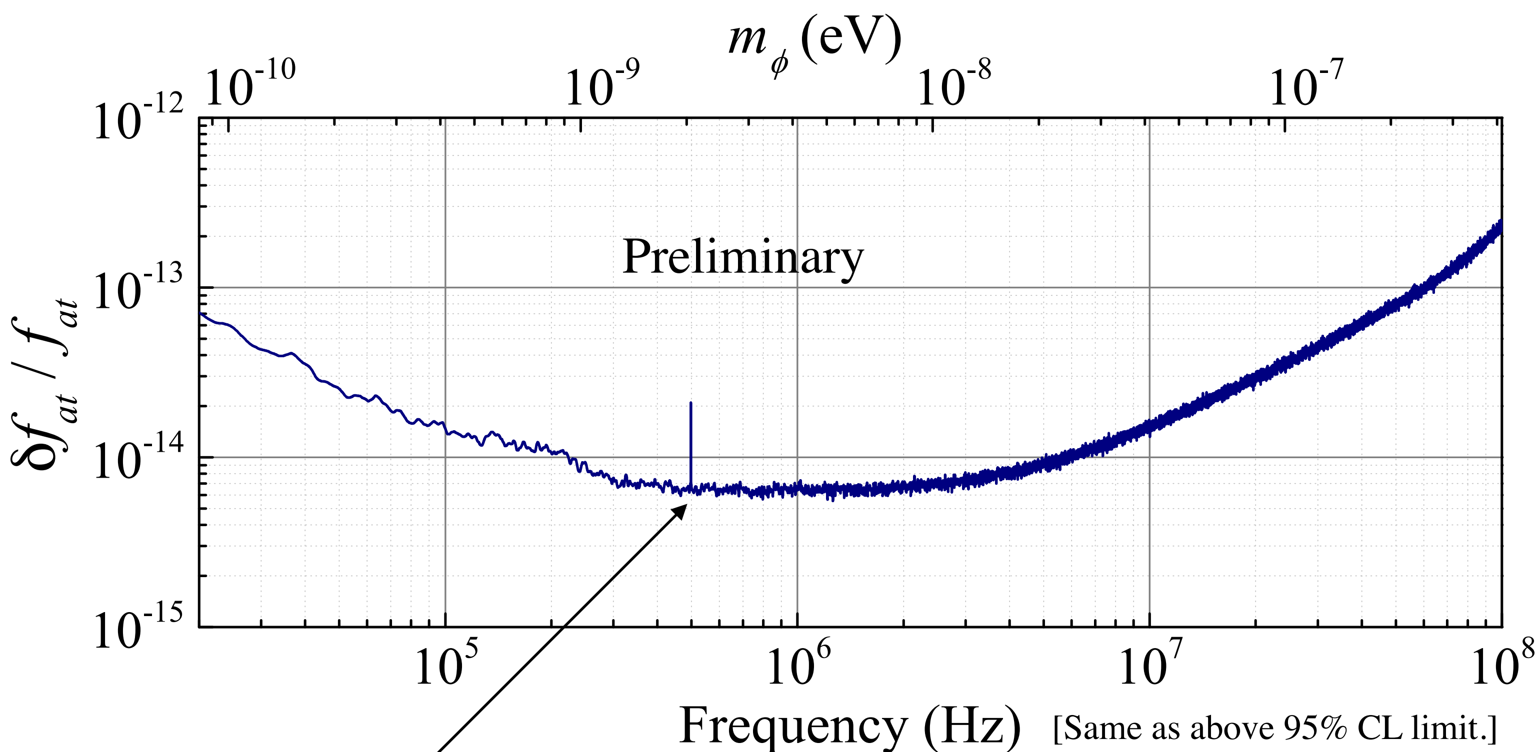

[Same as above 95% CL limit.]

3rd laser harmonics.

Beyond 1Hz DM mass \w polarization spectroscopy

Antypas, Tretiak, Garcon, Ozeri, GP & Budker, to appear

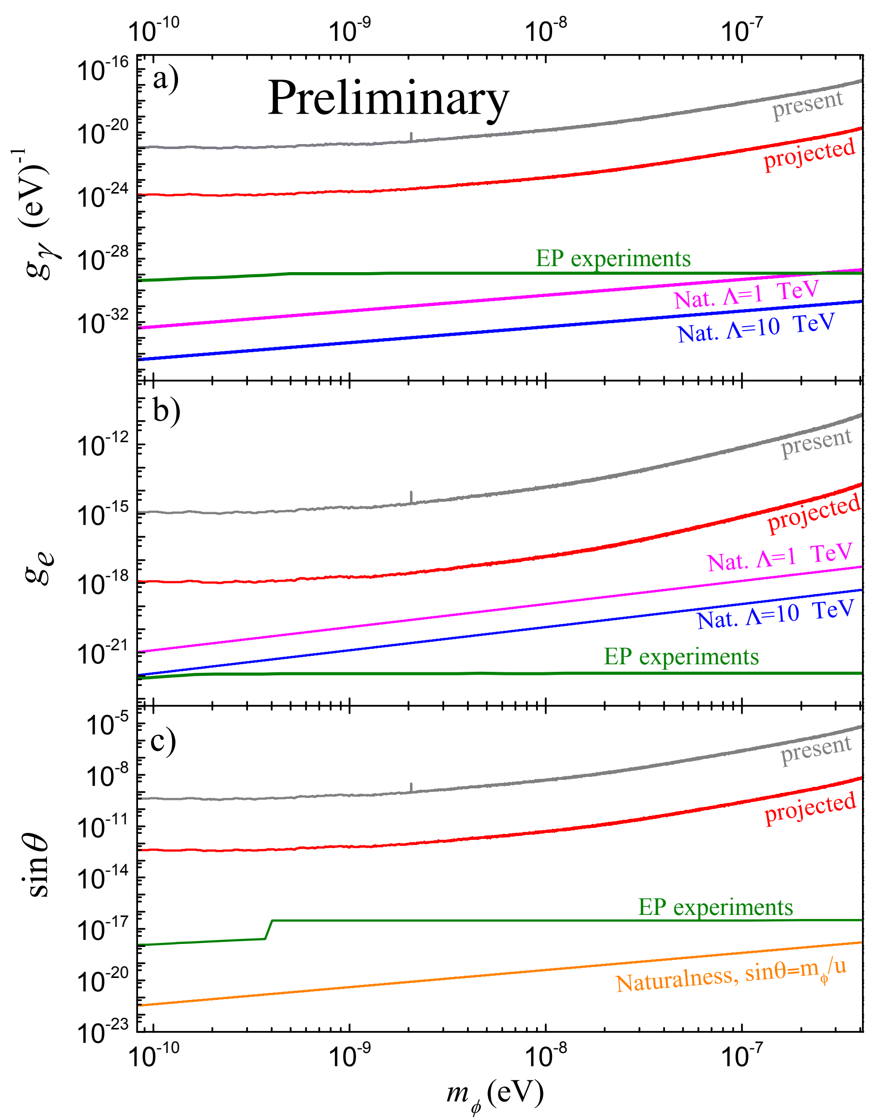

Relaxion’s Earth & Solar halos vs tabletops

Banerjee, Budker, Eby, Kim & GP (19)

Searching for a relaxion DM planet around us

Assume small DM density & large radius => mass-radii relation:

$$R_{\rm star} \approx \frac{M_{\rm Pl}^2}{m_\phi^2}\frac{1}{M_{\rm Earth}} \qquad (M_* \ll M_{\rm Earth})\,.$$

Eby, Leembruggen, Street, Suranyi & Wijewardhana (18);

Banerjee, Budker, Eby, Kim & GP (19)

Can obtain large density enhancement:

$$r \equiv \frac{\rho_{\rm star}}{\rho_{\rm loc-DM}} \sim \xi \frac{M_{\rm Earth}^4\, m_\phi^6}{M_{\rm Pl}^6\, \rho_{\rm loc-DM}} \sim \xi \times 10^{28} \times \left(\frac{m_\phi}{10^{-10}}\right)^6$$

$$\xi \equiv M_{\rm star}/M_{\rm Earth}$$

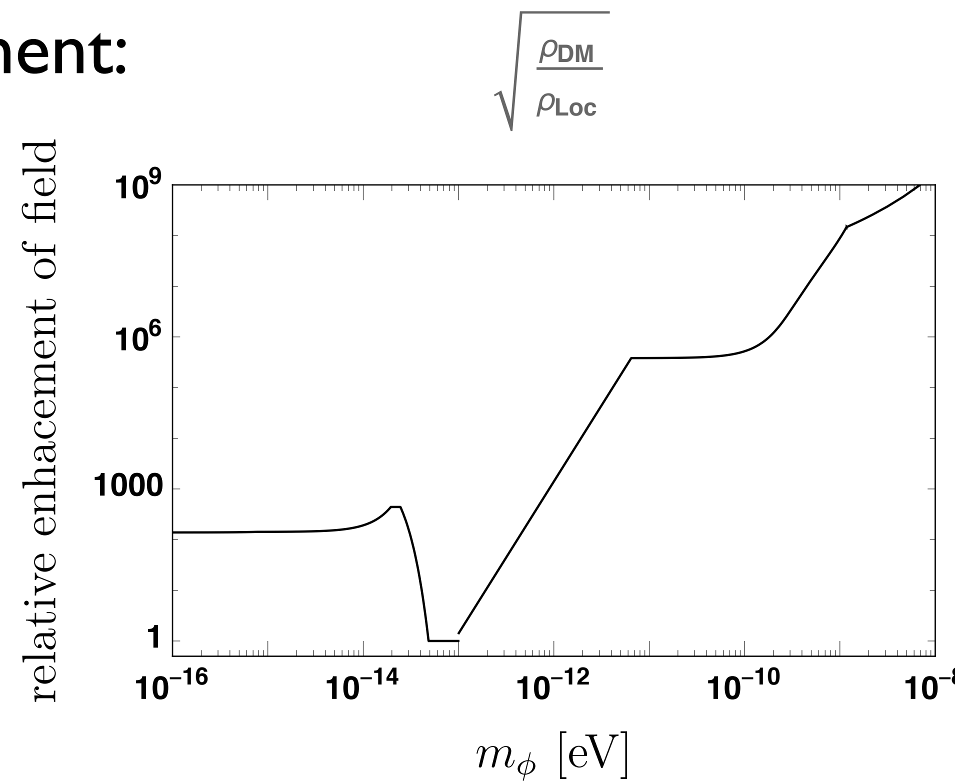

Other constraints max’ allowed mass

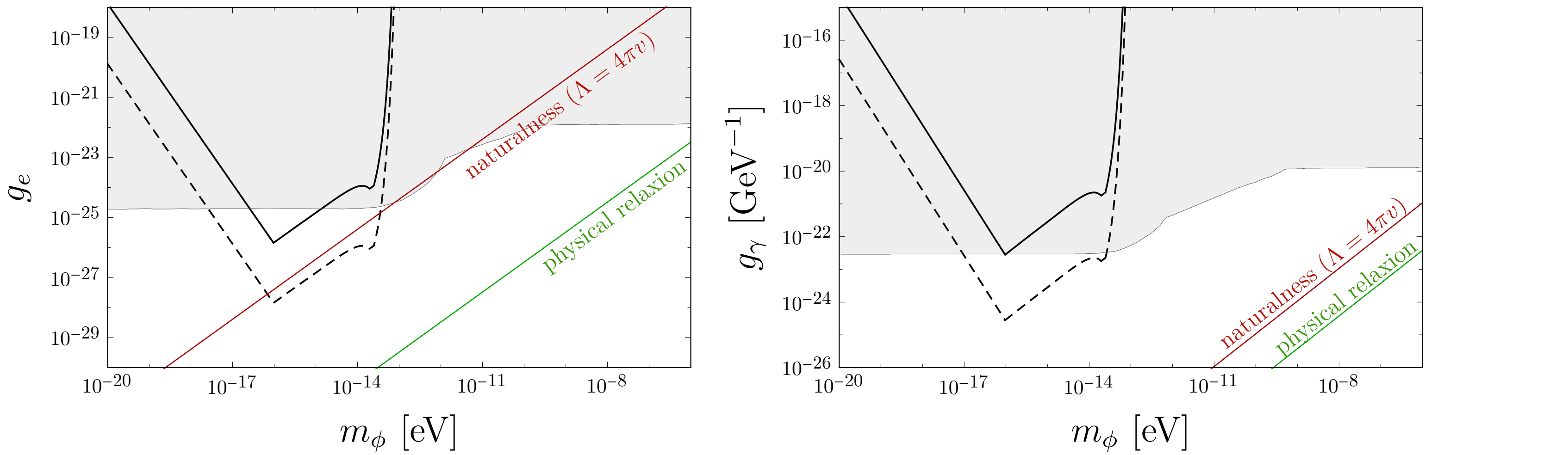

Solar halo: projected constraints on for a relaxion Solar halo. Experimental sensitivities = 10^{16}, 10^{18} (solid and dashed lines, respectively). The gray shaded region is excluded by EP. The red line is the naturalness limit, cutoff = 3 TeV, green line is an upper limit on coupling constants which can be obtained from physical relaxion models. The halo mass is taken as $M_? = \min[(M/2)(R_?/R)^3, (M_?)_{max}]$

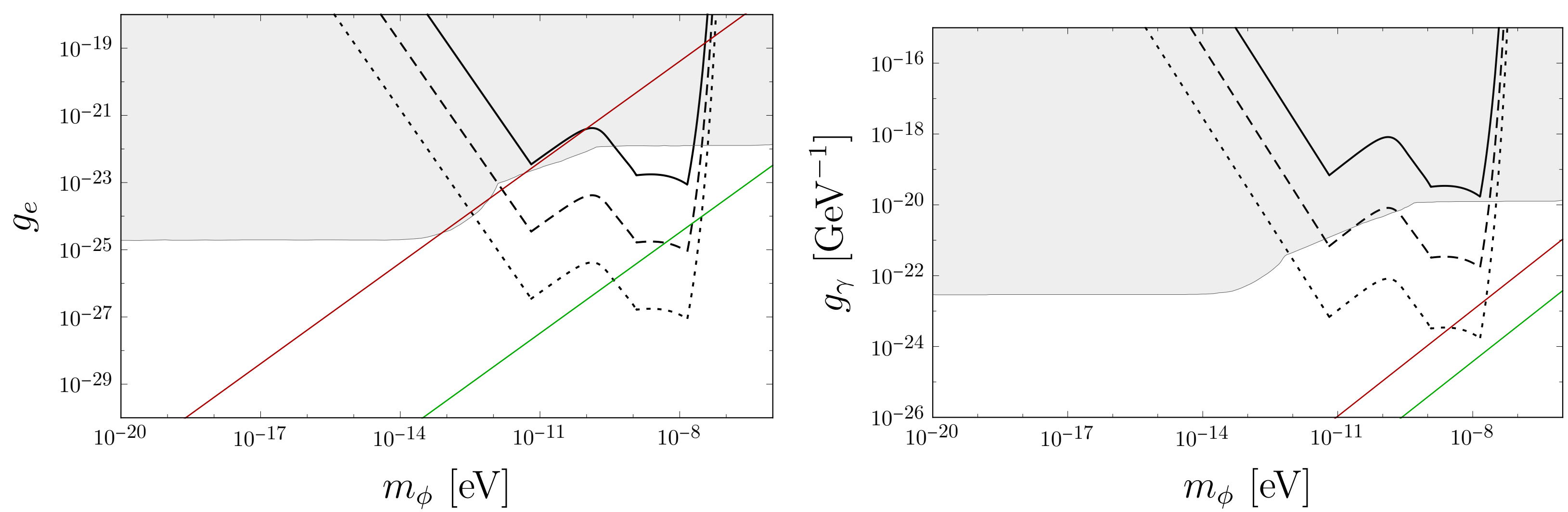

Earth halo: as above sensitivities = 10^{14},10^{16}, 10^{18}.

Conclusions

- Null-LHC + new paradigms + incredible sensitivity => new era!
- Relaxion-benchmarking allows to compare sensitivities.
- Relaxion-DM: dynamic decoupling -> strong bounds but cannot compete \w 5th force & can't probe physical region.
- Relaxion-DM-stars: table-top probe physical region, stronger than 5th force & can/should compare \w space.
- Interesting implications for ALP searches (GNOME & others).

Backups

Beyond 1Hz DM mass \w polarization spectroscopy

Antypas, Tretiak, Garcon, Ozeri, GP & Budker, to appear

Cs $6S_{1/2} \rightarrow 6P_{3/2}$ transition frequency (10 GHz)

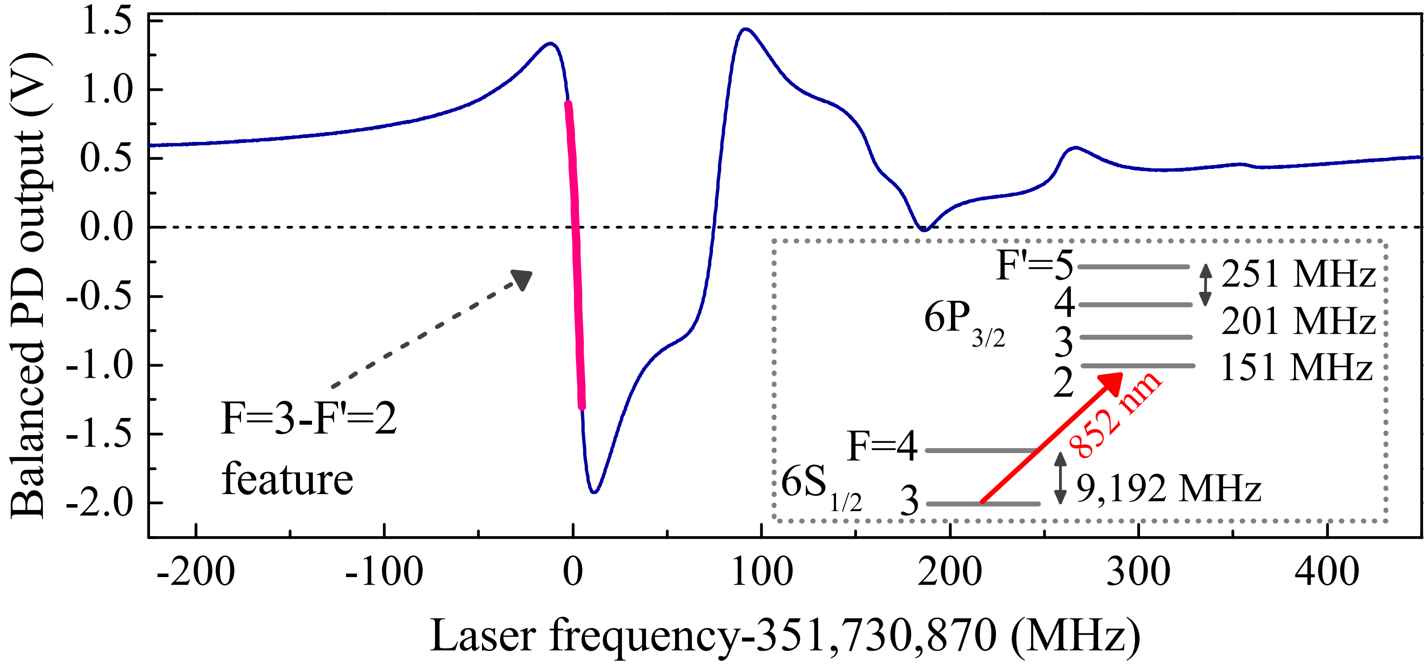

Other constraints max' allowed mass

Aharony, Akerman, Ozeri, GP & Shaniv & Savoray, in prep. (ion-cavity comparison); Banerjee, Budker, Eby, Kim, GP, in Prep.

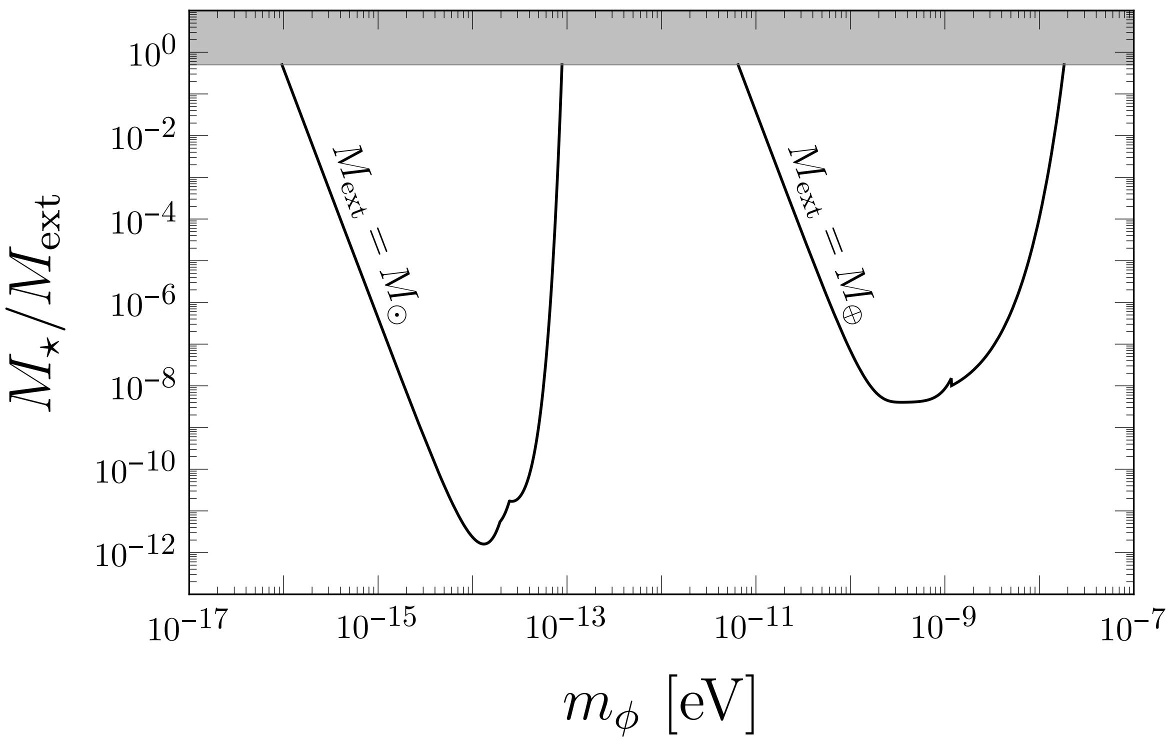

FIG. 2: The upper bound $(M_\star)_{\rm max}$ on the relaxion halo mass $M_\star$ as a function of scalar particle mass m_ϕ; the regions above the black lines are excluded by either (right side, assuming an Earth halo) lunar laser ranging [39], or (left side, assuming a Solar halo) planetary ephemerides [40]. We also require $M_\star \leq M_{\rm ext}/2$ (boundary of gray shaded region), as explained in the Supplementary Material S2.

Very interesting implications to GNOME

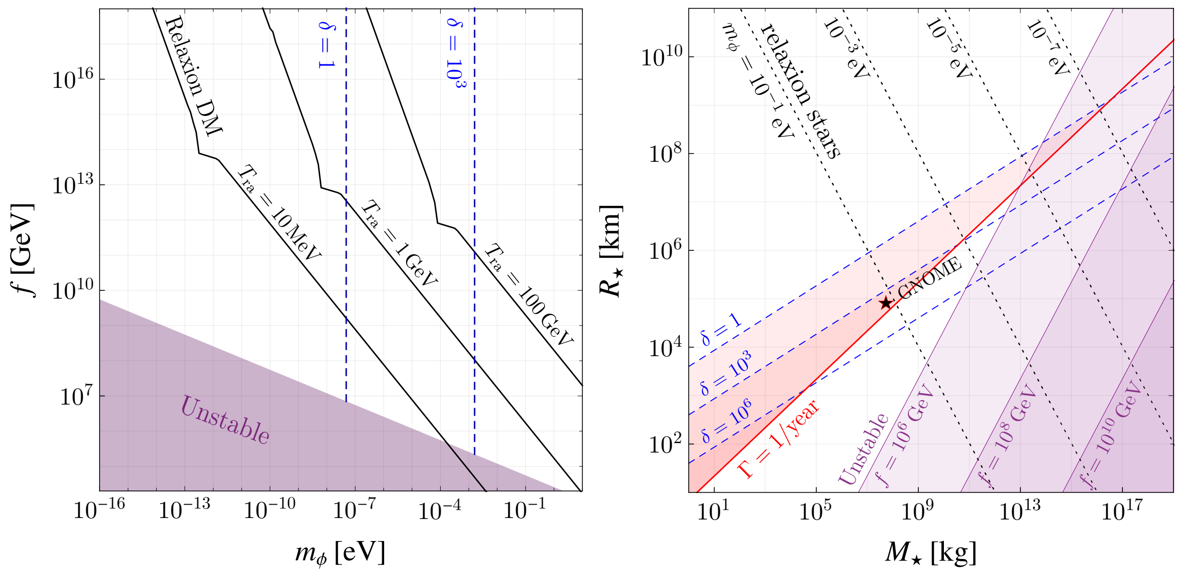

FIG. 1: The relevant parameter space for transient DM boson stars encountering the Earth. In both panels, the dashed blue lines are contours of constant overdensity δ, and the purple shaded regions indicate instability through self-interactions. Left: parameter space in scalar mass m_ϕ and decay constant f allowing for gravitationally stable objects, assuming $\Gamma = 1$/year; black lines denote the relaxion DM model of [9] for different choices of $T_{\rm ra}$, the cosmological temperature at which the relaxion backreaction potential reappears. Right: $M_\star$ and $R_\star$ are treated as independent parameters; the black dotted lines denote stable configurations formed from scalars of mass m_ϕ, and the red shaded region represents $\Gamma > 1$/year and $\delta > 1$. The black star represents the benchmark point used by the GNOME collaboration [34].

Large star DM density => visible effect

Aharony, Akerman, Ozeri, GP & Shaniv & Savoray, in prep. (ion-cavity comparison); Banerjee, Budker, Eby, Kim, GP, in Prep.

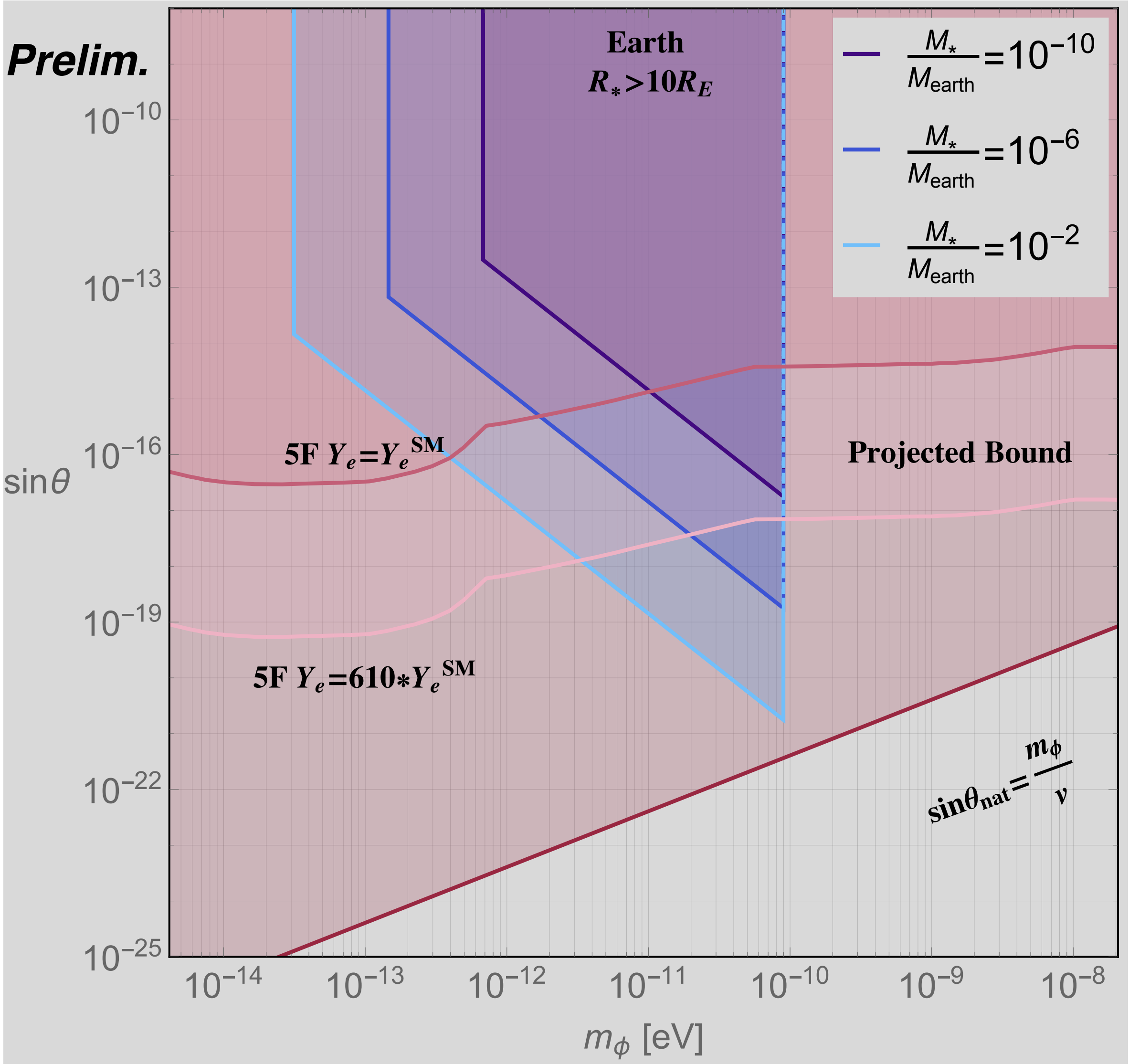

Large star DM density => visible effect

Aharony, Akerman, Ozeri, GP & Shaniv & Savoray, in prep. (ion-cavity comparison); Banerjee, Budker, Eby, Kim, GP, in Prep.

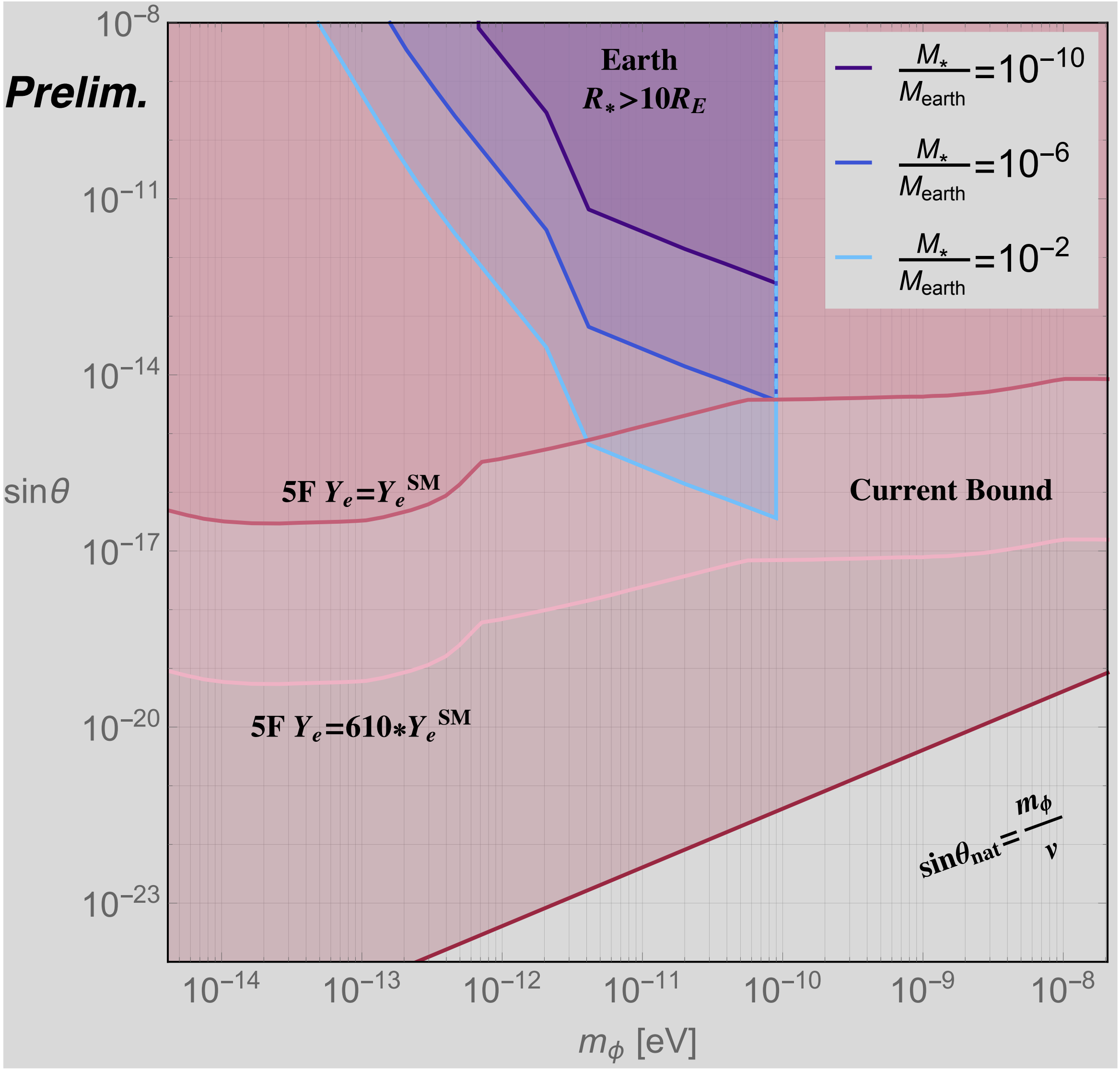

Subjective particle physicist perspective

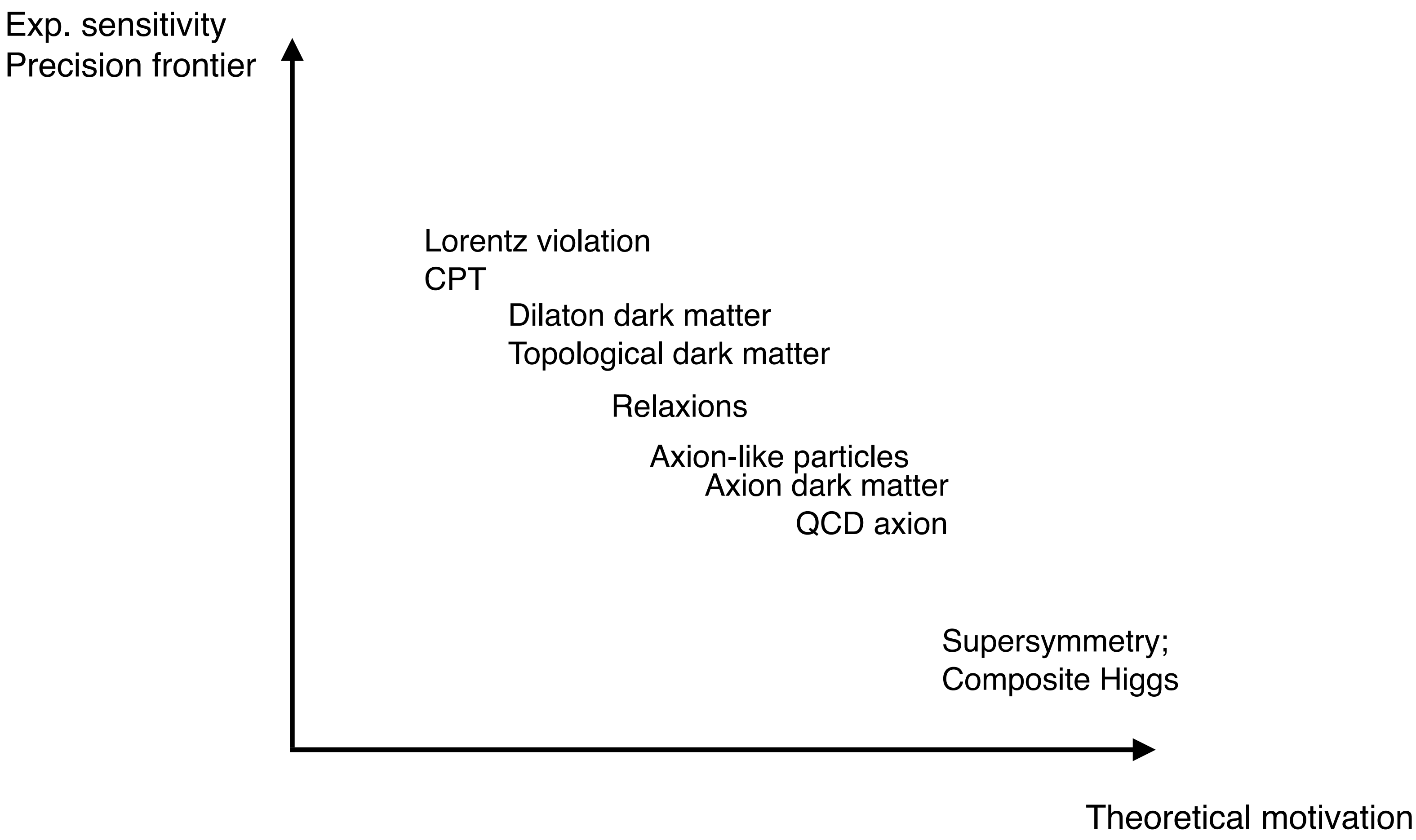

Beyond 1Hz DM mass \w dynamical decoupling

Aharony, Akerman, Ozeri, GP & Shaniv & Savoray, in prep.

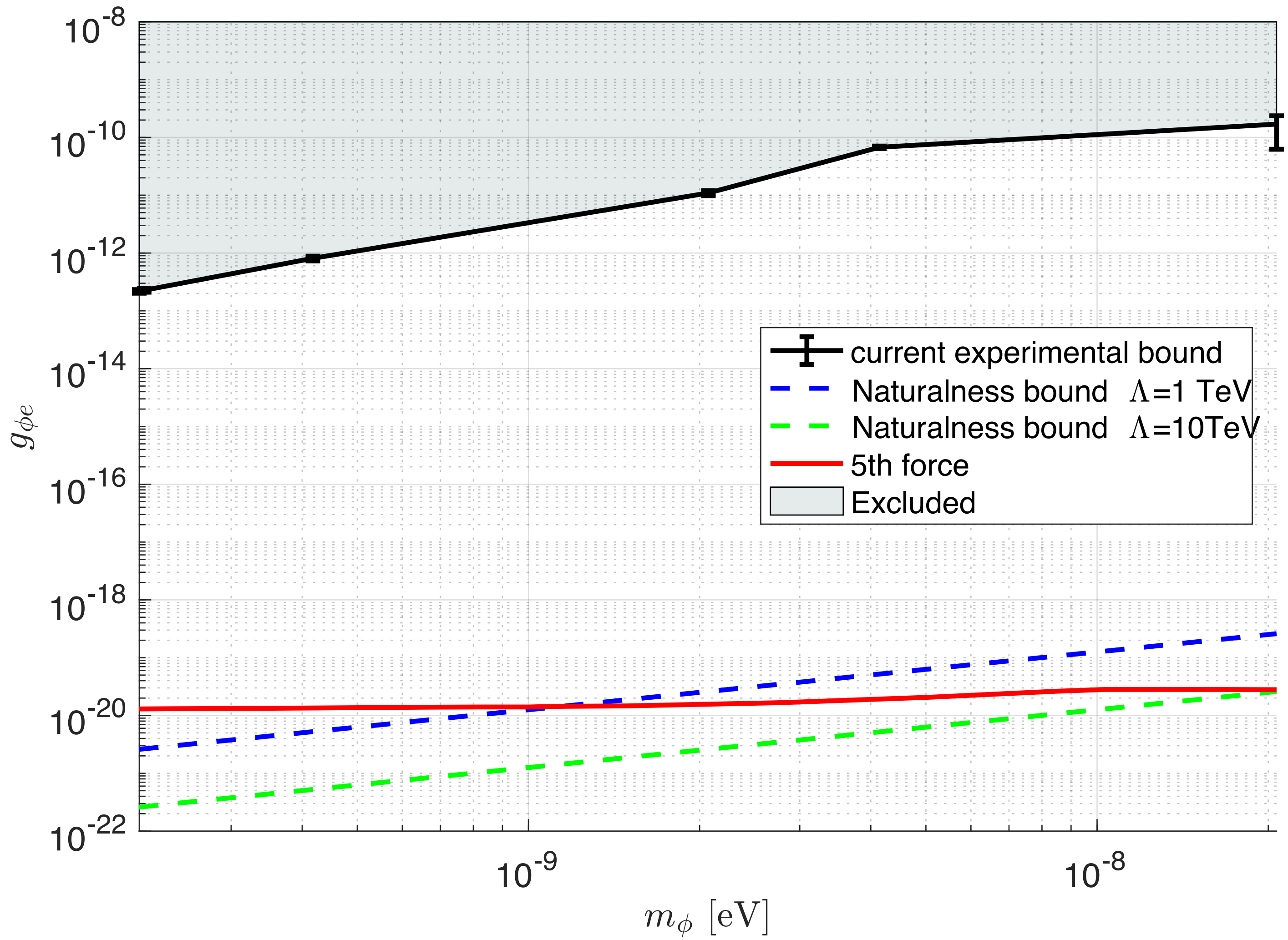

Beyond 1Hz DM mass \w dynamical decoupling

Aharony, Akerman, Ozeri, GP & Shaniv & Savoray, in prep.

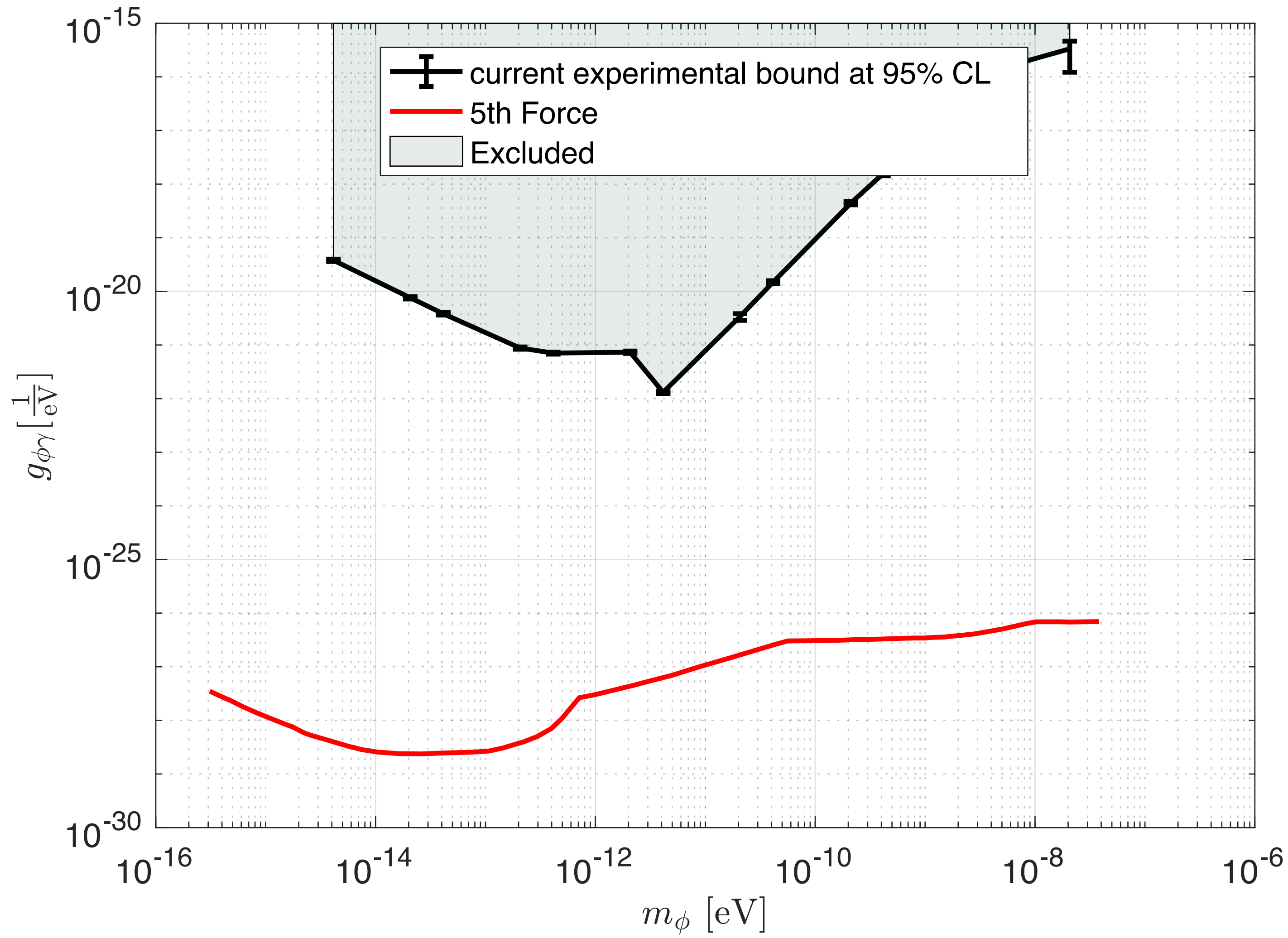

U(1)$_{B\text{-}L}$

Frugiuele, Fuchs, GP & Schlaffer (16)

Complementarity with astro/cosmo’ bounds:

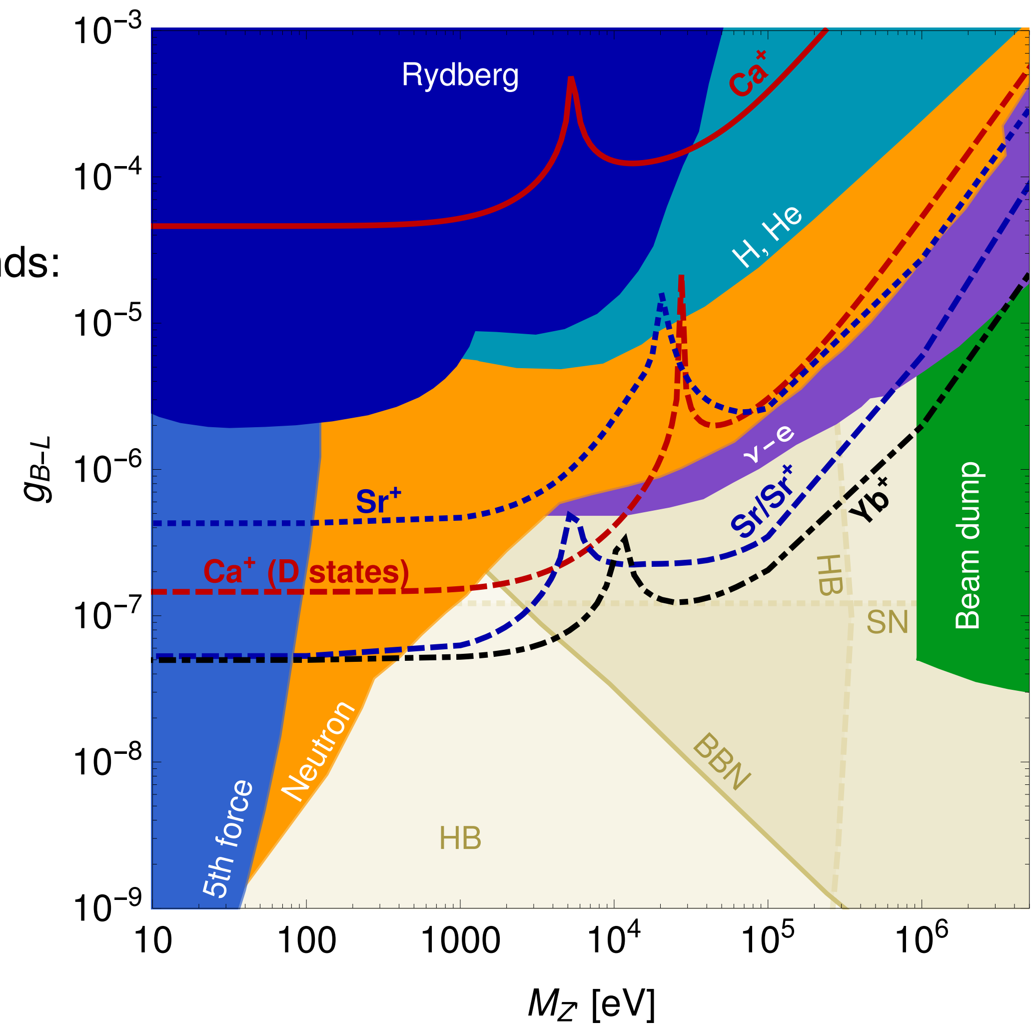

King comparison

- Level of linearity can be quantified by comparing area of triangle to that of a cube: $\mathrm{NL}/|\overrightarrow{m\nu}_2||\overrightarrow{m\nu}_1| \ll 1\,.$

$$\overrightarrow{m\mu} \equiv (1,1,1)\,.$$

$$\mathrm{NL} = \frac{1}{2}\,|(\overrightarrow{m\nu}_1 \times \overrightarrow{m\nu}_2)\cdot\overrightarrow{m\mu}|\,.$$

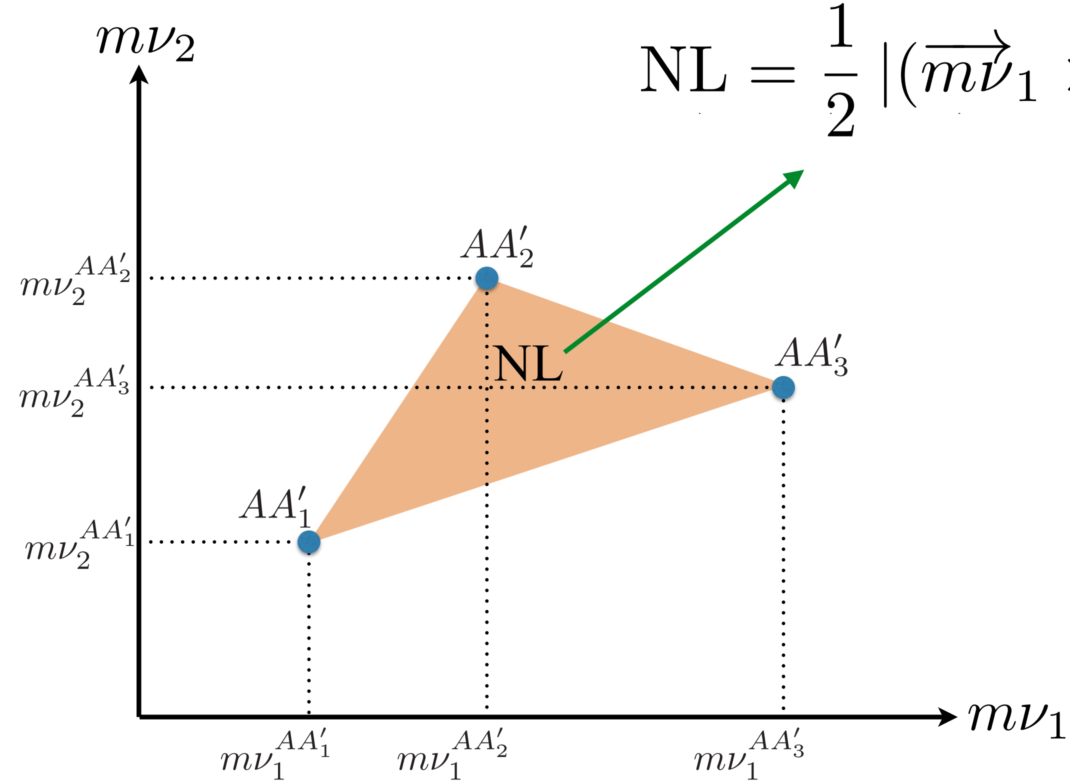

Or volume of prallelepiped:

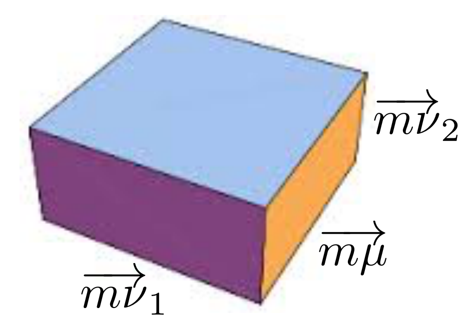

King linearity implications

♦ Linearity implies that $\overrightarrow{m\nu}_2$ & $\overrightarrow{m\nu}_1$ must be linearly dependent:

$$\overrightarrow{m\nu}_2 = K_2\,\overrightarrow{m_\mu} + F_2\,\vec{v} + \mathcal{O}\left(10^{-4}\right)$$
$$\overrightarrow{m\nu}_1 = K_1\,\overrightarrow{m_\mu} + F_1\,\vec{v} + \mathcal{O}\left(10^{-4}\right)$$

$$\overrightarrow{m\nu}_2 \cong K_{21}\,\overrightarrow{m\mu} + F_{21}\,\overrightarrow{m\nu}_1\,,$$

with $F_{21} \equiv F_2/F_1$ and $K_{21} \equiv K_2 - F_{21}K_1$.

F_i & $\vec{v}$ are unknown but F_{21} & K_{21} can be measured precisely.

Adding light new physics (NP)

New forces acts on electron & quarks leads to change of energy levels.

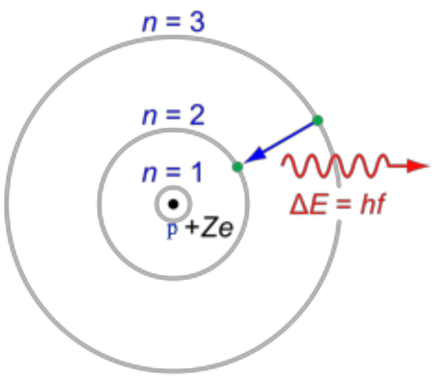

$$+ \quad \mathcal{L}_\phi = \phi(y_e \bar{e} e + y_n \bar{n} n) \quad \Longrightarrow$$

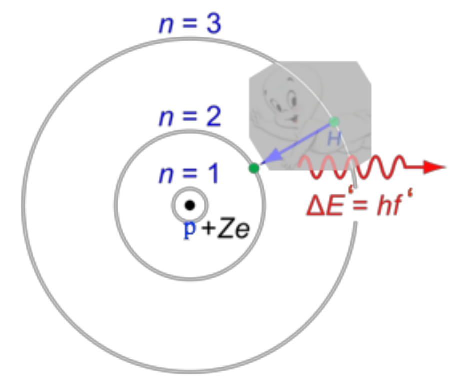

- New physics part known, precisely calculated:

CI+MBPT: Dzuba, Flambaum & Kozlov (96) Berengut, Flambaum & Kozlov (06);
GRASP2K: Jonsson, Gaigalas, Biero, Fischer & Grant (2013)

(Combination of the many-body perturbation theory with the configuration-interaction method)

$$\overrightarrow{m\nu}_i = K_i \, \overrightarrow{m_\mu} + F_i \, \vec{v} + \boxed{y_e y_n X_i \vec{h}},$$

Delaunay, Ozeri, GP & Soreq (16)

$$\Downarrow$$

$$\overrightarrow{m\nu}_2 = K_{21} \overrightarrow{m\mu} + F_{21} \overrightarrow{m\nu}_1 + \alpha_{\rm NP} \vec{h} X_1 \left(X_{21} - F_{21} \right) \, ,$$

and $X_{21} \equiv X_2 / X_1$.

Illustration: adding light new physics (NP)

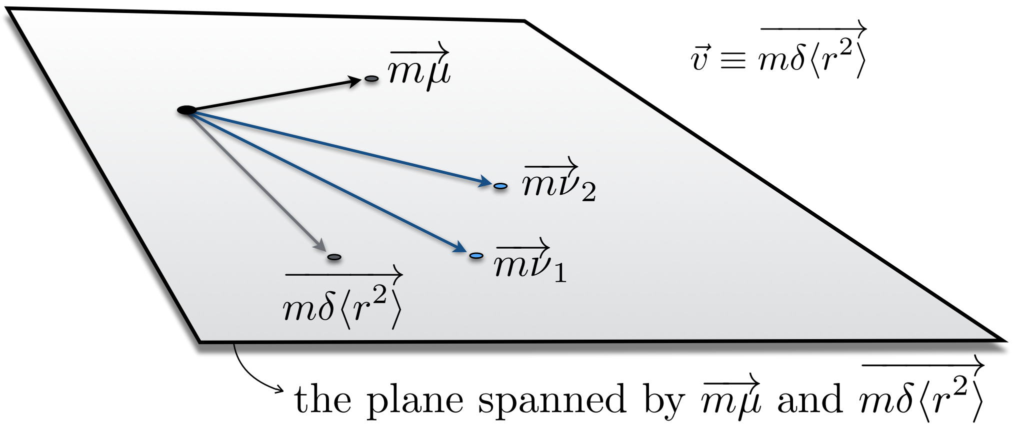

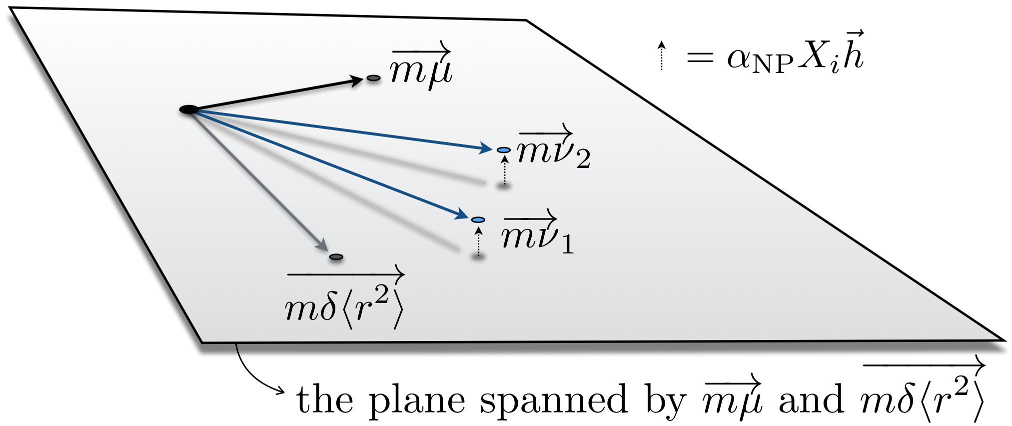

Light mediators

If mediator's mass, m_X, is smaller than inverse of outer electrons than the potential is Coulombic.

If mediator's mass is smaller than inverse distance of most inner electron from the nucleus then the full Yukawa potential is required.

Otherwise the potential is described via a delta function.

$$V(r) = \begin{cases} \frac{1}{r} \quad \text{for} \quad m_X \lesssim \alpha m_e \,, \\ \frac{e^{-r m_X}}{r} \quad \text{for} \quad \alpha m_e \lesssim m_X \lesssim \alpha m_e Z \,, \\ \frac{1}{m_X^2}\, \delta^3(r) \quad \text{otherwise} \,. \end{cases}$$

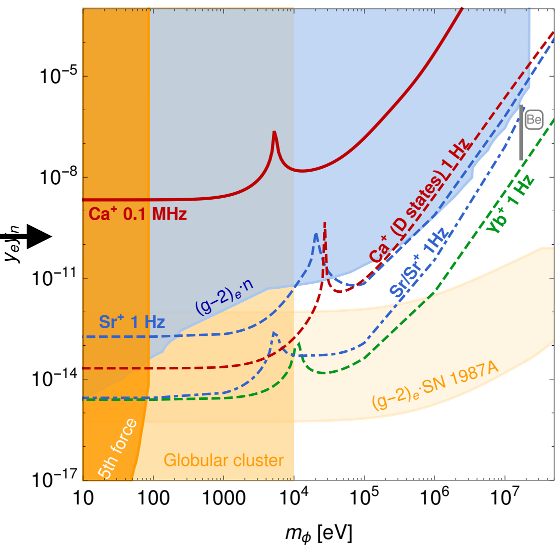

Be 17 MeV anomaly

Frugiuele, Fuchs, GP & Schlaffer v2 (16)

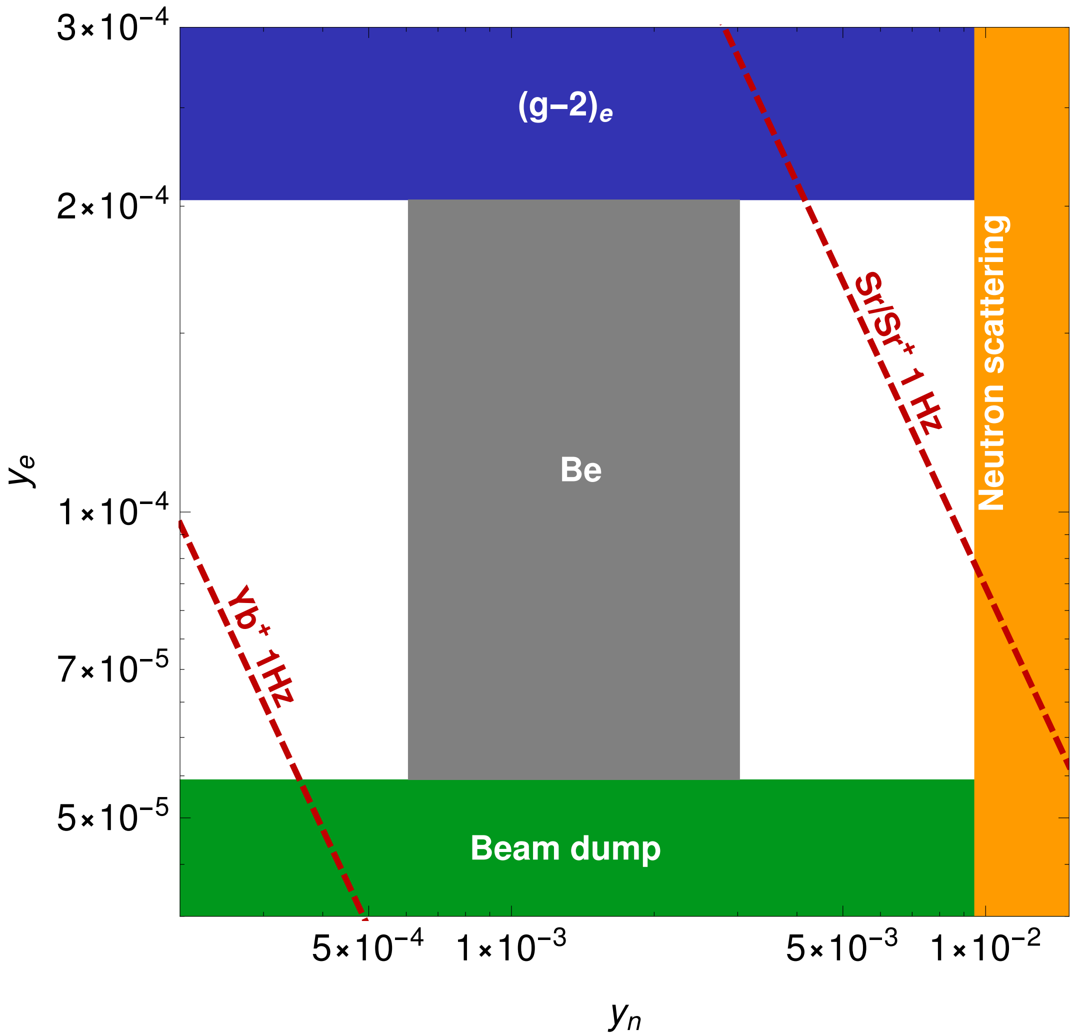

Ex.: Yb^+ with Z=70, n=6 and A=168(4)-174(6).

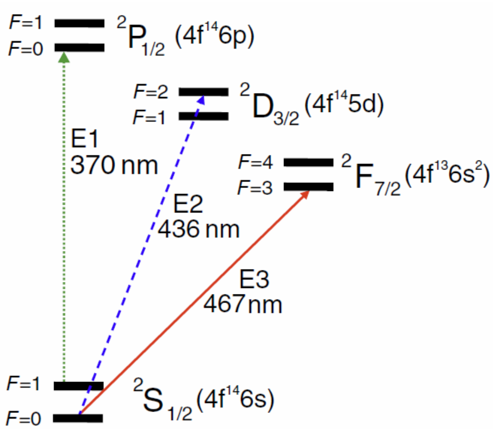

The Kossel shell structure of ytterbium.

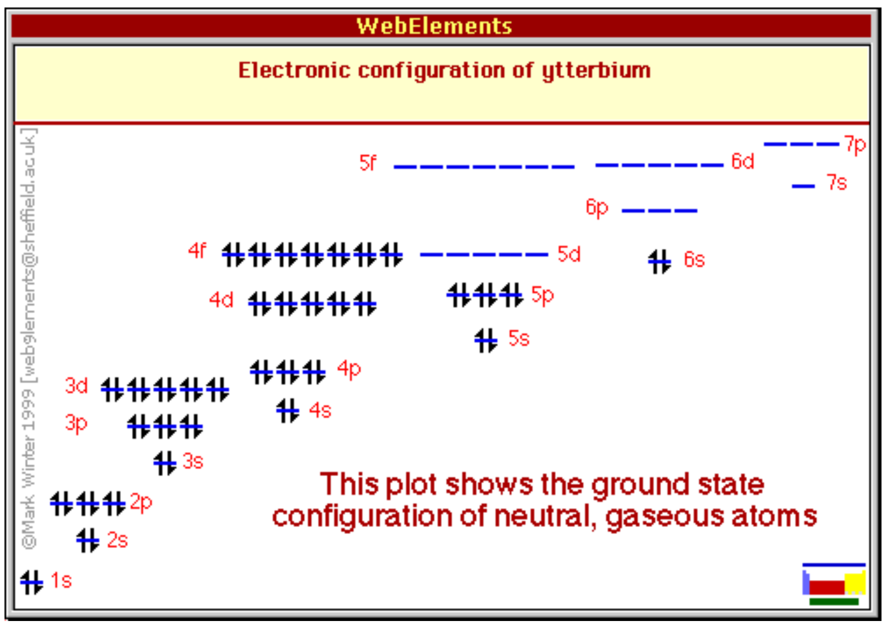

The electronic configuration of ytterbium.

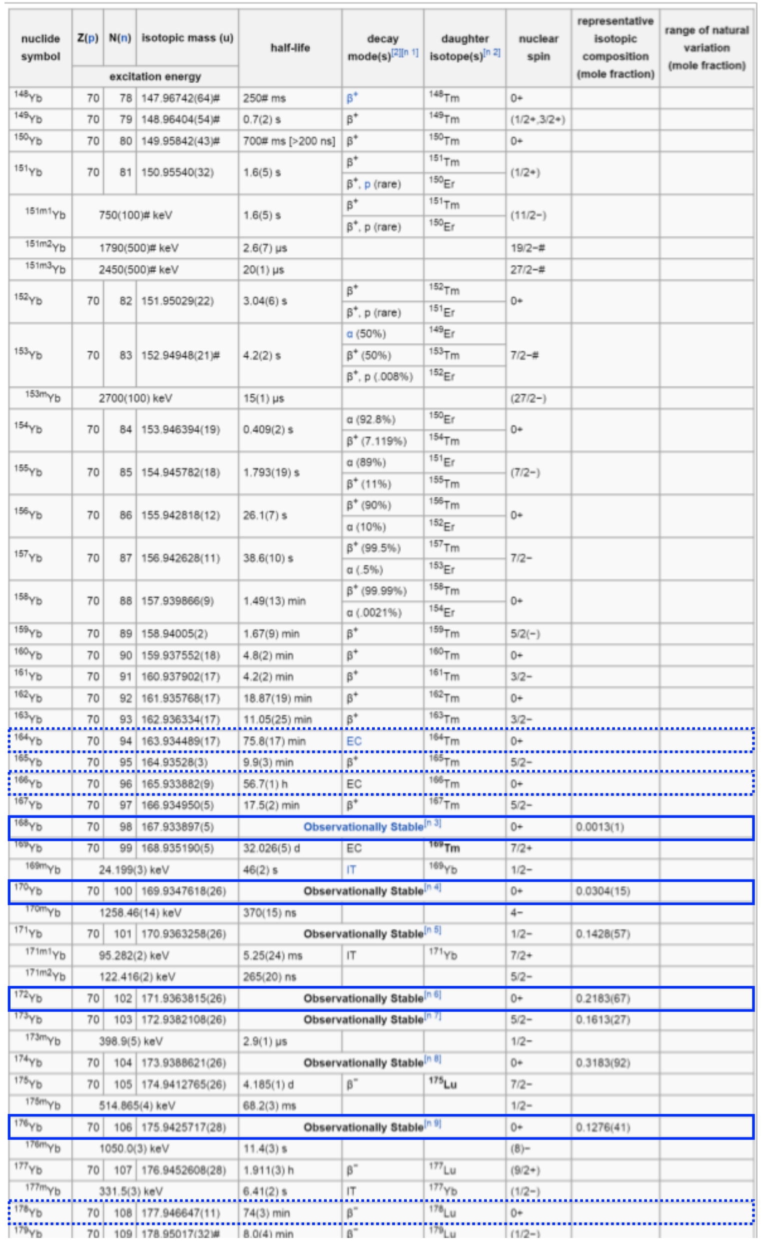

nuclide symbol	Z(p)	N(n)	isotopic mass (u)	half-life	decay mode(s)[2][n 1]	daughter isotope(s)[n 2]	nuclear spin	representative isotopic composition (mole fraction)	range of natural variation (mole fraction)
	excitation energy								
^{148}Yb	70	78	147.96742(64)#	250# ms	β^+	^{148}Tm	0+		
^{149}Yb	70	79	148.96404(54)#	0.7(2) s	β^+	^{149}Tm	(1/2+,3/2+)		
^{150}Yb	70	80	149.95842(43)#	700# ms [>200 ns]	β^+	^{150}Tm	0+		
^{151}Yb	70	81	150.95540(32)	1.6(5) s	β^+	^{151}Tm	(1/2+)		
					β^+, p (rare)	^{150}Er			
$^{151m1}Yb$	750(100)# keV			1.6(5) s	β^+	^{151}Tm	(11/2−)		
					β^+, p (rare)	^{150}Er			
$^{151m2}Yb$	1790(500)# keV			2.6(7) μs			19/2−#		
$^{151m3}Yb$	2450(500)# keV			20(1) μs			27/2−#		
^{152}Yb	70	82	151.95029(22)	3.04(6) s	β^+	^{152}Tm	0+		
					β^+, p (rare)	^{151}Er			
^{153}Yb	70	83	152.94948(21)#	4.2(2) s	α (50%)	^{149}Er	7/2−#		
					β^+ (50%)	^{153}Tm			
					β^+, p (.008%)	^{152}Er			
^{153m}Yb	2700(100) keV			15(1) μs			(27/2−)		
^{154}Yb	70	84	153.946394(19)	0.409(2) s	α (92.8%)	^{150}Er	0+		
					β^+ (7.119%)	^{154}Tm			
^{155}Yb	70	85	154.945782(18)	1.793(19) s	α (89%)	^{151}Er	(7/2−)		
					β^+ (11%)	^{155}Tm			
^{156}Yb	70	86	155.942818(12)	26.1(7) s	β^+ (90%)	^{156}Tm	0+		
					α (10%)	^{152}Er			
^{157}Yb	70	87	156.942628(11)	38.6(10) s	β^+ (99.5%)	^{157}Tm	7/2−		
					α (.5%)	^{153}Er			
^{158}Yb	70	88	157.939866(9)	1.49(13) min	β^+ (99.99%)	^{158}Tm	0+		
					α (.0021%)	^{154}Er			
^{159}Yb	70	89	158.94005(2)	1.67(9) min	β^+	^{159}Tm	5/2(−)		
^{160}Yb	70	90	159.937552(18)	4.8(2) min	β^+	^{160}Tm	0+		
^{161}Yb	70	91	160.937902(17)	4.2(2) min	β^+	^{161}Tm	3/2−		
^{162}Yb	70	92	161.935768(17)	18.87(19) min	β^+	^{162}Tm	0+		
^{163}Yb	70	93	162.936334(17)	11.05(25) min	β^+	^{163}Tm	3/2−		
^{164}Yb	70	94	163.934489(17)	75.8(17) min	EC	^{164}Tm	0+		
^{165}Yb	70	95	164.93528(3)	9.9(3) min	β^+	^{165}Tm	5/2−		
^{166}Yb	70	96	165.933882(9)	56.7(1) h	EC	^{166}Tm	0+		
^{167}Yb	70	97	166.934950(5)	17.5(2) min	β^+	^{167}Tm	5/2−		
^{168}Yb	70	98	167.933897(5)	Observationally Stable[n 3]			0+	0.0013(1)	
^{169}Yb	70	99	168.935190(5)	32.026(5) d	EC	^{169}Tm	7/2+		
^{169m}Yb	24.199(3) keV			46(2) s	IT	^{169}Yb	1/2−		
^{170}Yb	70	100	169.9347618(26)	Observationally Stable[n 4]			0+	0.0304(15)	
^{170m}Yb	1258.46(14) keV			370(15) ns			4−		
^{171}Yb	70	101	170.9363258(26)	Observationally Stable[n 5]			1/2−	0.1428(57)	
$^{171m1}Yb$	95.282(2) keV			5.25(24) ms	IT	^{171}Yb	7/2+		
$^{171m2}Yb$	122.416(2) keV			265(20) ns			5/2−		
^{172}Yb	70	102	171.9363815(26)	Observationally Stable[n 6]			0+	0.2183(67)	
^{173}Yb	70	103	172.9382108(26)	Observationally Stable[n 7]			5/2−	0.1613(27)	
^{173m}Yb	398.9(5) keV			2.9(1) μs			1/2−		
^{174}Yb	70	104	173.9388621(26)	Observationally Stable[n 8]			0+	0.3183(92)	
^{175}Yb	70	105	174.9412765(26)	4.185(1) d	β^-	^{175}Lu	7/2−		
^{175m}Yb	514.865(4) keV			68.2(3) ms			1/2−		
^{176}Yb	70	106	175.9425717(28)	Observationally Stable[n 9]			0+	0.1276(41)	
^{176m}Yb	1050.0(3) keV			11.4(3) s			(8)−		
^{177}Yb	70	107	176.9452608(28)	1.911(3) h	β^-	^{177}Lu	(9/2+)		
^{177m}Yb	331.5(3) keV			6.41(2) s	IT	^{177}Yb	(1/2−)		
^{178}Yb	70	108	177.946647(11)	74(3) min	β^-	^{178}Lu	0+		
^{179}Yb	70	109	178.95017(32)#	8.0(4) min	β^-	^{179}Lu	(1/2−)		

Precision mass measurements: 10^{-10}

Contents lists available at ScienceDirect

International Journal of Mass Spectrometry

journal homepage: www.elsevier.com/locate/ijms

The most precise atomic mass measurements in Penning traps

Edmund G. Myers*

Florida State University, Department of Physics, Tallahassee, FL 32306-4350, USA

Table 10
Atomic masses of the most abundant isotopes of strontium and ytterbium measured at FSU [109].

Atom	FSU mass (u)	σ_m/m (ppt)
^{86}Sr	85.909 260 730 9(91)	105
^{87}Sr	86.908 877 497 0(91)	105
^{88}Sr	87.905 612 257 1(97)	110
^{170}Yb	169.934 767 241(18)	105
^{171}Yb	170.936 331 514(19)	110
^{172}Yb	171.936 386 655(18)	105
^{173}Yb	172.938 216 213(18)	105
^{174}Yb	173.938 867 539(18)	105
^{176}Yb	175.942 574 702(22)	125

Partial solution, comparing different isotope shift, searching of nonlinearity in "King plot"

King's factorisation formula (King, 1963):

only depend on e-transition

$$\delta\nu_i^{AA'} \equiv \nu_i^A - \nu_i^{A'} = K_i\,\mu_{AA'} + F_i\delta\langle r^2\rangle_{AA'}\,,$$

($\mu_{AA'} \equiv 1/m_A - 1/m_{A'} = (A' - A)/(AA')\,\mathrm{amu}^{-1}$, where amu $\approx 0.931\,\mathrm{GeV}$)

only depend on nucleus

We can solve for $\delta\langle r^2\rangle_{AA'}$ to get a linear relation:

$$m\delta\nu^2_{AA'} = F_{21} m\delta\nu^1_{AA'} + K_{21}\,,$$

(with $K_{21} \equiv (K_2 - F_{21}K_1)$ and $F_{21} \equiv F_2/F_1$ and $m\delta\nu^i_{AA'} \equiv \delta\nu^i_{AA'}/\mu_{AA'}$.)

Ex.: Yb^+ with Z=70, n=6 and A=168(4)-174(6).

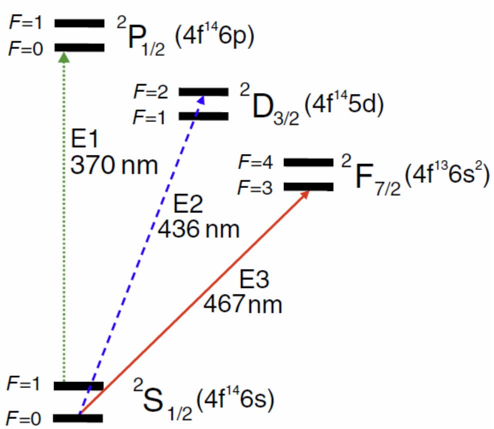

The Kossel shell structure of ytterbium.

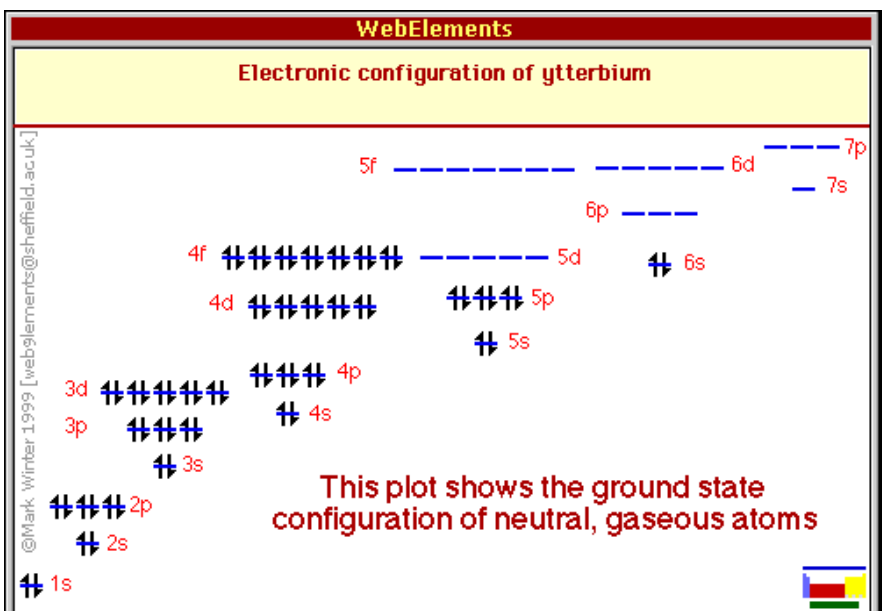

The electronic configuration of ytterbium.

nuclide symbol	Z(p)	N(n)	isotopic mass (u) / excitation energy	half-life	decay mode(s)[2][n 1]	daughter isotope(s)[n 2]	nuclear spin	representative isotopic composition (mole fraction)	range of natural variation (mole fraction)
^{148}Yb	70	78	147.96742(64)#	250# ms	β^+	^{148}Tm	0+		
^{149}Yb	70	79	148.96404(54)#	0.7(2) s	β^+	^{149}Tm	(1/2+,3/2+)		
^{150}Yb	70	80	149.95842(43)#	700# ms [>200 ns]	β^+	^{150}Tm	0+		
^{151}Yb	70	81	150.95540(32)	1.6(5) s	β^+	^{151}Tm	(1/2+)		
					β^+, p (rare)	^{150}Er			
^{151m1}Yb			750(100)# keV	1.6(5) s	β^+	^{151}Tm	(11/2−)		
					β^+, p (rare)	^{150}Er			
^{151m2}Yb			1790(500)# keV	2.6(7) μs			19/2−#		
^{151m3}Yb			2450(500)# keV	20(1) μs			27/2−#		
^{152}Yb	70	82	151.95029(22)	3.04(6) s	β^+	^{152}Tm	0+		
					β^+, p (rare)	^{151}Er			
^{153}Yb	70	83	152.94948(21)#	4.2(2) s	α (50%)	^{149}Er	7/2−#		
					β^+ (50%)	^{153}Tm			
					β^+, p (.008%)	^{152}Er			
^{153m}Yb			2700(100) keV	15(1) μs			(27/2−)		
^{154}Yb	70	84	153.946394(19)	0.409(2) s	α (92.8%)	^{150}Er	0+		
					β^+ (7.119%)	^{154}Tm			
^{155}Yb	70	85	154.945782(18)	1.793(19) s	α (89%)	^{151}Er	(7/2−)		
					β^+ (11%)	^{155}Tm			
^{156}Yb	70	86	155.942818(12)	26.1(7) s	β^+ (90%)	^{156}Tm	0+		
					α (10%)	^{152}Er			
^{157}Yb	70	87	156.942628(11)	38.6(10) s	β^+ (99.5%)	^{157}Tm	7/2−		
					α (.5%)	^{153}Er			
^{158}Yb	70	88	157.939866(9)	1.49(13) min	β^+ (99.99%)	^{158}Tm	0+		
					α (.0021%)	^{154}Er			
^{159}Yb	70	89	158.94005(2)	1.67(9) min	β^+	^{159}Tm	5/2(−)		
^{160}Yb	70	90	159.937552(18)	4.8(2) min	β^+	^{160}Tm	0+		
^{161}Yb	70	91	160.937902(17)	4.2(2) min	β^+	^{161}Tm	3/2−		
^{162}Yb	70	92	161.935768(17)	18.87(19) min	β^+	^{162}Tm	0+		
^{163}Yb	70	93	162.936334(17)	11.05(25) min	β^+	^{163}Tm	3/2−		
^{164}Yb	70	94	163.934489(17)	75.8(17) min	EC	^{164}Tm	0+		
^{165}Yb	70	95	164.93528(3)	9.9(3) min	β^+	^{165}Tm	5/2−		
^{166}Yb	70	96	165.933882(9)	56.7(1) h	EC	^{166}Tm	0+		
^{167}Yb	70	97	166.934950(5)	17.5(2) min	β^+	^{167}Tm	5/2−		
^{168}Yb	70	98	167.933897(5)	Observationally Stable[n 3]			0+	0.0013(1)	
^{169}Yb	70	99	168.935190(5)	32.026(5) d	EC	^{169}Tm	7/2+		
^{169m}Yb			24.199(3) keV	46(2) s	IT	^{169}Yb	1/2−		
^{170}Yb	70	100	169.9347618(26)	Observationally Stable[n 4]			0+	0.0304(15)	
^{170m}Yb			1258.46(14) keV	370(15) ns			4−		
^{171}Yb	70	101	170.9363258(26)	Observationally Stable[n 5]			1/2−	0.1428(57)	
^{171m1}Yb			95.282(2) keV	5.25(24) ms	IT	^{171}Yb	7/2+		
^{171m2}Yb			122.416(2) keV	265(20) ns			5/2−		
^{172}Yb	70	102	171.9363815(26)	Observationally Stable[n 6]			0+	0.2183(67)	
^{173}Yb	70	103	172.9382108(26)	Observationally Stable[n 7]			5/2−	0.1613(27)	
^{173m}Yb			398.9(5) keV	2.9(1) μs			1/2−		
^{174}Yb	70	104	173.9388621(26)	Observationally Stable[n 8]			0+	0.3183(92)	
^{175}Yb	70	105	174.9412765(26)	4.185(1) d	β^-	^{175}Lu	7/2−		
^{175m}Yb			514.865(4) keV	68.2(3) ms			1/2−		
^{176}Yb	70	106	175.9425717(28)	Observationally Stable[n 9]			0+	0.1276(41)	
^{176m}Yb			1050.0(3) keV	11.4(3) s			(8)−		
^{177}Yb	70	107	176.9452608(28)	1.911(3) h	β^-	^{177}Lu	(9/2+)		
^{177m}Yb			331.5(3) keV	6.41(2) s	IT	^{177}Yb	(1/2−)		
^{178}Yb	70	108	177.946647(11)	74(3) min	β^-	^{178}Lu	0+		
^{179}Yb	70	109	178.95017(32)#	8.0(4) min	β^-	^{179}Lu	(1/2−)		

Ex.: $Sr^{(+)}$ with Z=38, n=5 and A=84-88 (90).

- **Electron Configuration:** $1s^2$ $2s^2p^6$ $3s^2p^6d^{10}$ $4s^2p^6$ $5s^{2(1)}$
- **Electrons per Energy Level:** 2,8,18,8,2(1)

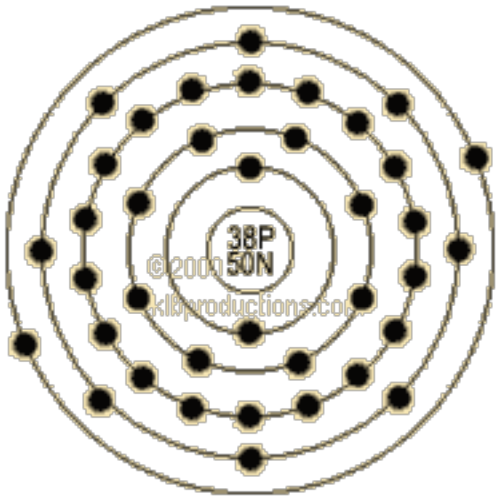

Ex.: $Ca^{(+)}$ with Z=20, n=4 and A=40-48.

- **Electron Configuration:** $1s^2\ 2s^2p^6\ 3s^2p^6\ 4s^1$
- **Electrons per Energy Level:** 2,8,8,2(1)
-

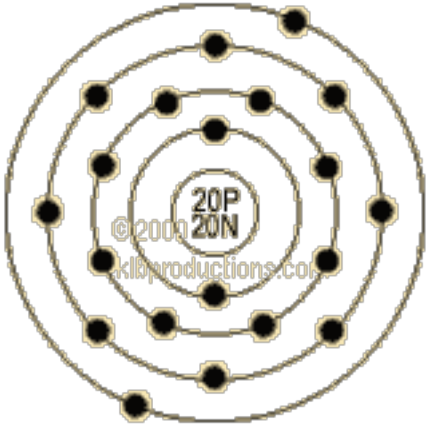

Ex.: Dy with Z=66, n=6 and A=158-164.

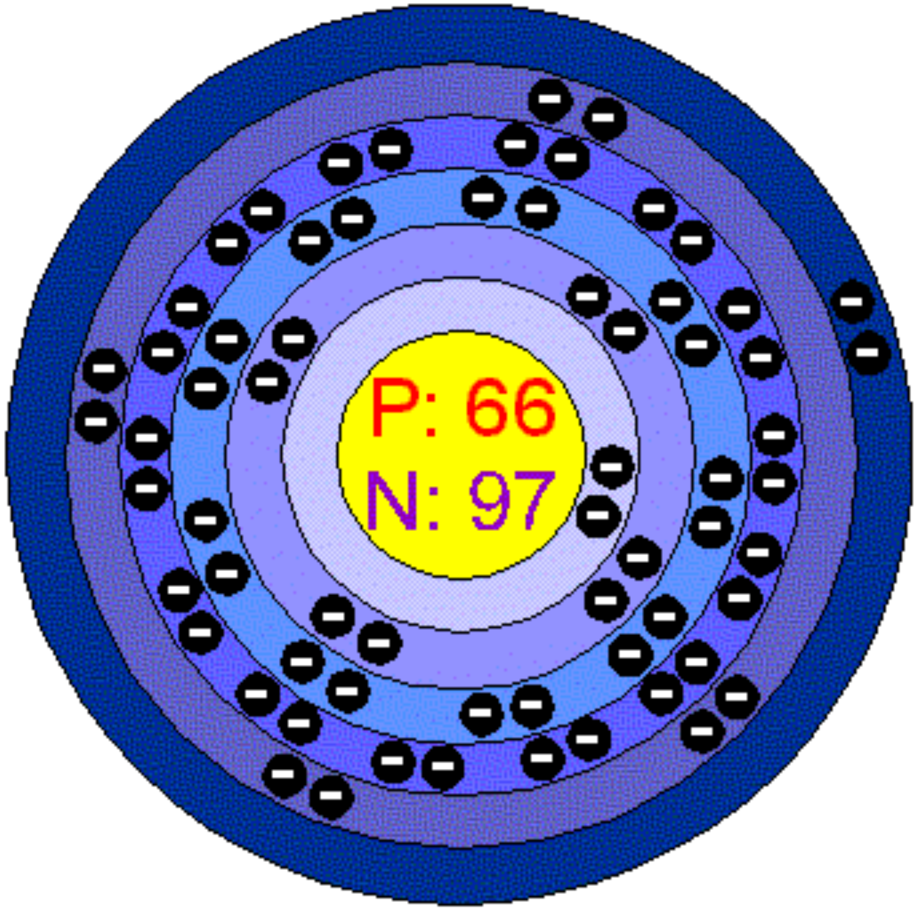

Number of Energy Levels: 6
First Energy Level: 2
Second Energy Level: 8
Third Energy Level: 18
Fourth Energy Level: 28
Fifth Energy Level: 8
Sixth Energy Level: 2

The observables

- We have 3 isotope shifts $(AA'_{1,2,3})$ for 2 transitions (i=1,2):

$$\overrightarrow{m\nu}_i \equiv \left(m\nu_i^{AA'_1}, m\nu_i^{AA'_2}, m\nu_i^{AA'_3} \right)$$

$$\nu_i^{AA'} \equiv \nu_i^{A} - \nu_i^{A'} . \qquad m\nu_i^{AA'} \equiv \nu_i^{AA'} / \mu_{AA'}$$

$$\mu_{AA'} \equiv m_A^{-1} - m_{A'}^{-1}$$

Target accuracy: $\Delta m\nu_i^{AA'} / m\nu_i^{AA'} \lesssim 10^{-6}$.
(currently: 10^{-4}, projected $< 10^{-9}$)

The observable: King comparison (1964)

- What would be the generic form of $\overrightarrow{m\nu}_2$ vs. $\overrightarrow{m\nu}_1$?
- 3 ISs - $m\nu_2 = am\nu_1^2 + bm\nu_1 + c$:

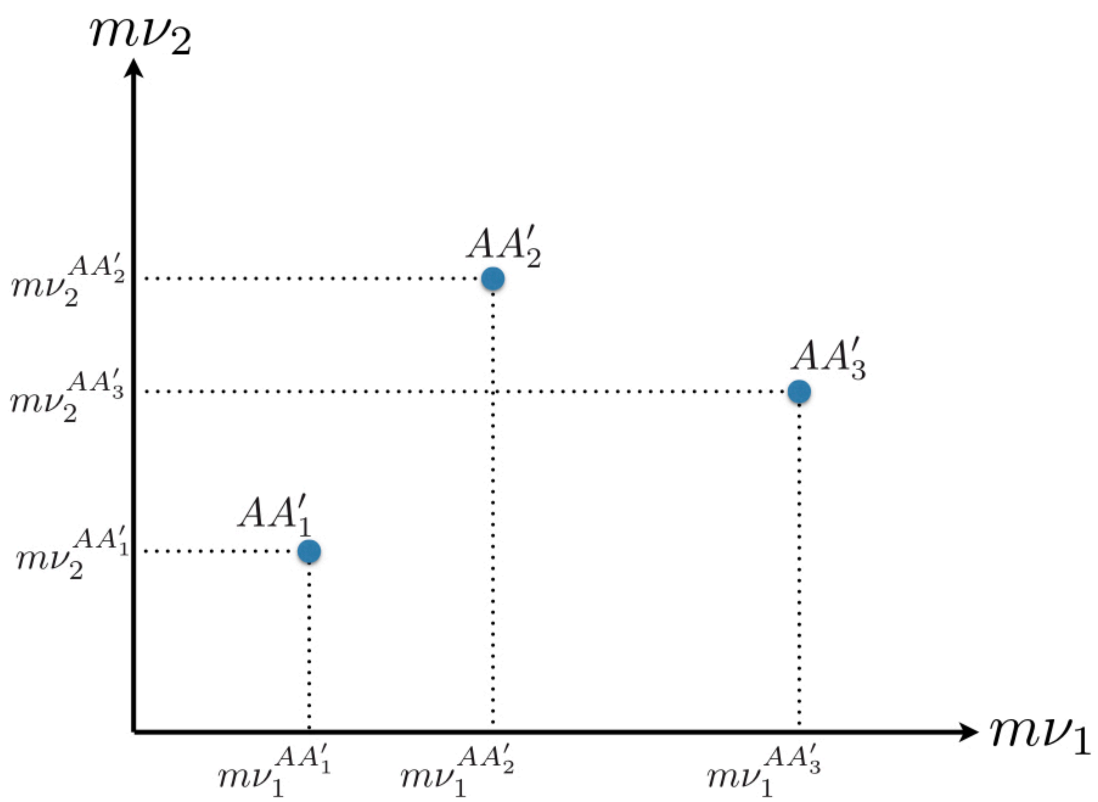

What about existing data ?

Limitation of method

$$\alpha_{\rm NP} = \frac{(\overrightarrow{m\nu}_1 \times \overrightarrow{m\nu}_2)\cdot \overrightarrow{m\mu}}{(\overrightarrow{m\mu}\times\vec{h})\cdot(X_1\,\overrightarrow{m\nu}_2 - X_2\,\overrightarrow{m\nu}_1)}$$

Berengut, Budker, Delaunay, Flambaum, Frugiuele, Fuchs, Grojean, Harnik, Ozeri, GP & Soreq (17)

- Only useful to bound new physics (barring cancellation).

- Short range NP: $X_i \propto F_i \;\Rightarrow\; \vec{v}$ is redefined to absorb NP; requires extra carefulness when approaching this limit.

- As long as linearity holds bounds are limited by exp' accuracy:

$$\alpha_{\rm NP} \lesssim \sigma_{\alpha_{\rm NP}} = \sqrt{\Sigma_k(\partial\alpha_{\rm NP}/\partial O_k)^2\sigma_k^2}\,,$$

$(O_K$ various exp' observables.)

- Once non-linearity observed bound will be set by observation.